Electronic Supplementary Material (ESI) for Nanoscale.

Supporting Information

Tuning the Catalytic Activity and Selectivity of Water-Soluble Bimetallic RuPt Nanoparticles by Modifying their Surface Metal Distribution

Donia Bouzouita,[1] Guy Lippens,[2] Edwin A. Baquero,[3] Pier F. Fazzini,[1] Gregory Pieters,[4] Yannick Coppel,[5] Pierre Lecante,[6] Simon Tricard,[1,] Luis M. Martínez-Prieto[1,*] and Bruno Chaudret[1,*]*

[1] LPCNO, Laboratoire de Physique et Chimie des Nano-Objets, UMR5215 INSA-CNRS UPS, Institut des Sciences appliquées, 135, Avenue de Rangueil, F-31077 Toulouse, France.

[2] LISBP, Université de Toulouse, CNRS, INRA, INSA, UPS 135 avenue de Rangueil, 31077 Toulouse, France.

[3] Departamento de Química, Facultad de Ciencias Universidad Nacional de Colombia, Sede Bogotá Carrera 30 No. 45-03, 111321, Bogotá, Colombia.

[4] SCBM, CEA, Univ. Paris Saclay, F-91191, Gif-sur-Yvette, France.

[5] CNRS, LCC (Laboratoire de Chimie de Coordination), Universit´e de Toulouse, UPS, INPT, 205 route de Narbonne, BP 44099, F-31077-Toulouse Cedex 4, France.

[6] CEMES (Centre d'Elaboration de Matériaux et d'Etudes Structurales), CNRS, 29 Rue J. Marvig, F-31055 Toulouse, France.

Table of contents

S1. Experimental Section

General considerations and starting materials

All chemical operations were carried out under an argon atmosphere using standard Schlenk, Fisher-Porter reactors and glove-box techniques. Solvents were purified before use: THF and pentane were collected from a MBraun purification system.

Ru(COD)(COT) and $Pt(NBE)_3$ were purchased from Nanomeps Toulouse, $Pt(CH_3)_2(COD)$ from STREM, CO and D_2 gas from Air liquide, ^{13}CO (^{13}C, 99.14%) from Eurisotop, L-lysine (98%) and $Pt_2(dba)_3$ from Sigma-Aldrich. All reagents were used as received from the commercial sources.

Elemental Analysis were performed by Thermogravimetric analyses (TGA) with a TGA/DSC 1 STAR System equipped with an ultra-microbalance UMX5, a gas switch GC200 and DTA and DSC sensors. The samples were analyzed through a two-step oxidation/reduction method. First the sample was heated from 25 °C to 700 °C at 10 °C/min under air (2h). After cooling down, it was heated again from 25 °C to 900 °C at 30 °C/min under a gas mixture Ar/H_2 4% (3h).

Wide-angle X-ray scattering (WAXS). WAXS was performed at CEMES-CNRS. Samples were sealed in 1.0 mm diameter Lindemann glass capillaries. The samples were irradiated with graphite monochromatized molybdenum Kα (0.071069 nm) radiation and the X-ray intensity scattered measurements were performed using a dedicated two-axis diffractometer. Radial distribution functions (RDF) were obtained after Fourier transformation of the reduced intensity functions.

Nuclear Magnetic Resonance (NMR). ^1H spectra were recorded on a Bruker Avance 400 MHz spectrometer. NMR tubes were prepared under argon atmosphere and monitored at 55 °C during 16 h for the kinetic experiments.

Solid state NMR (MAS-NMR). Solid-state NMR experiments were recorded at the LCC (Toulouse) on a Bruker Avance 400 MHz spectrometer equipped with 2.5 mm probes. Samples were spun between 16 to 20 kHz at the magic angle using ZrO_2 rotors. ^{13}C MAS experiments were performed with a recycle delay of 20 s. ^{13}C CP/MAS spectra were recorded with a recycle delay of 2 s and a contact time of 4 ms. Hahn-echo scheme were synchronized with the spinning rate.

Transmission Electron Microscopy (TEM) and High resolution TEM (HRTEM). The NPs were observed by TEM and HRTEM after deposition of a drop of a solution of the isolated nanoparticles after dispersion in THF on a copper grid covered with amorphous carbon. TEM analyses were performed at the UMS-Castaing by using a JEOL JEM 1400 electron microscope operating at 120 kV. The

approximation of the particles mean size was made through a manual analysis of enlarged micrographs by measuring 300 particles on a given grid.

HRTEM observations were performed using a Probe Corrected JEOL JEM-ARM200F Cold FEG equipped with a High Angle EDX detector working at 200 kV.

Scanning Electron Microscopy – Energy dispersive XRay spectroscopie (SEM-EDX). Scanning electron microscopy with energy dispersive X-ray spectroscopy (SEM/EDS) was performed on a JEOL JSM 7800F operated at 10 kV with a thermally assisted Schottky electron gun and equipped with a Bruker XFlash 6|60 detector (silicon drift detector technology). Samples for SEM/EDS analysis were prepared by pressing powder of NPs@SILPs on carbon tape.

Infrared spectroscopy (IR). ATR IR-FT spectra were recorded on a Thermo Scientific Nicolet 6700 spectrometer in the range 4000-600 cm^{-1}.

High-performance liquid chromatography (HPLC): HPLC chromatograms were recorded using a Phenomonex chiral column [3126 (D)-penicillamine (ref 00F-3126-E0); 25 cm × 4.6 mm]. Mobile phase: 2mM $CuSO_4$. Flow rate: 1.0 $ml.min^{-1}$. T^a: 22 °C. detector: UV at 254 nm.

Synthesis of Ru, Pt and RuPt NPs

Ru NPs were synthesized according to the procedure described in the literature:[1] Typically, a Schlenk flask was charged with **PrIPr** (34.7 mg, 0.099 mmol, 0.25 equiv.) and KO*t*Bu (12.2 mg, 0.109 mmol). The solids were suspended in THF (30 mL) and stirred at r.t. for 20 h. The resulting solution (yellow-orange) was transferred under an argon atmosphere into a 250 mL Fisher-Porter bottle charged with a frozen solution (-80 °C) of Ru(COD)(COT) (125 mg, 0.395 mmol, 1 equiv.) in 30 mL of THF (previously degassed). The Fisher-Porter reactor was pressurized with 3 bar of H_2, the solution was stirred for 20 hours at r.t. leading to a black homogeneous solution. After that, the remaining H_2 pressure was evacuated, the solution was concentrated to 2-3 mL, and 30 mL of pentane were added. The resulting black precipitate was washed with pentane (50 mL) and dried overnight under vacuum. TGA measurements gave the following Pt content: 53 %. Yield: 64mg, 84%.

Pt NPs: A Schlenk flask was charged with **PrIPr** (68.8 mg, 0.196 mmol, 0.25 equiv.) and KO*t*Bu (24.2 mg, 0.216 mmol). The solids were suspended in THF (30 mL) and stirred at r.t. for 20 h. The resulting solution (yellow-orange) was transferred under an argon atmosphere into a 250 mL Fisher-Porter bottle charged with a frozen solution (-80 °C) of $Pt(NBE)_3$ (375 mg, 0.785 mmol, 1 equiv.) in 30 mL of

[1] L. M. Martinez-Prieto, E. A. Baquero, G. Pieters, J. C. Flores, E. de Jesus, C. Nayral, F. Delpech, P. W. N. M. van Leeuwen, G. Lippens and B. Chaudret, *Chem. Commun.* **2017**, *53*, 5850-5853.

THF (previously degassed). The Fisher-Porter reactor was pressurized with 3 bar of H_2, the solution was stirred for 20 hours at r.t. leading to a black homogeneous solution. After that, the remaining H_2 pressure was evacuated, the solution was concentrated to 2-3 mL, and 30 mL of pentane were added. The resulting black precipitate was washed with pentane (50 mL) and dried overnight under vacuum. TGA measurements gave the following Pt content: 76 %. Yield: 120mg, 60 %.

RuPt-nor: A Schlenk flask was charged with **PrIPr** (28.11 mg, 0.08 mmol, 0.25 equiv.) and KO*t*Bu (9.87 mg, 0.088 mmol). The solids were suspended in THF (30 mL) and stirred at r.t. for 20 h. The resulting solution (yellow-orange) was transferred under argon atmosphere into a 250 mL Fisher-Porter bottle charged with a frozen solution (-80 °C) of Ru(COD)(COT) (50 mg, 0.16 mmol, 0.5 equiv.) and $Pt(NBE)_3$ (76.4 mg, 0.16 mmol, 0.5 equiv.) in 30 mL of THF (previously degassed). The Fischer-Porter reactor was pressurized with 3 bar of H_2, and the solution was stirred for 20 h at r.t. leading to a black homogeneous solution. After that, the remaining H_2 pressure was evacuated, the solution was concentrated to 2-3 mL, and 30 mL of pentane were added. The resulting black precipitate was washed with pentane (50 mL) and dried overnight under vacuum. TGA measurements gave the following metal content: 72 %. Yield: 50 mg, 78 %.

RuPt-DMC: A Schlenk flask was charged with **PrIPr** (28.11 mg, 0.08 mmol, 0.25 equiv.) and KO*t*Bu (9.87 mg, 0.088 mmol). The solids were suspended in THF (30 mL) and stirred at r.t. for 20 h. The resulting solution (yellow-orange) was transferred under argon atmosphere into a 250 mL Fisher-Porter bottle charged with a frozen solution (-80 °C) of Ru(COD)(COT) (50 mg, 0.16 mmol, 0.5 equiv.) and $Pt(CH_3)_2(COD)$ (53.33 mg, 0.16 mmol, 0.5 equiv.) in 30 mL of THF (previously degassed). The Fischer-Porter reactor was pressurized with 3 bar of H_2, and the solution was stirred for 20 h at r.t leading to a black homogeneous solution. After that, the remaining H_2 pressure was evacuated, the solution was concentrated to 2-3 mL, and 30 mL of pentane were added. The resulting black precipitate was washed with pentane (50 mL) and dried overnight under vacuum. TGA gave the following metal content: 68 %. Yield: 50 mg, 81 %.

RuPt-dba: A Schlenk flask was charged with **PrIPr** (28.11 mg, 0.08 mmol, 0.25 equiv.) and KO*t*Bu (9.87 mg, 0.088 mmol). The solids were suspended in THF (30 mL) and stirred at r.t. for 20 h. The resulting solution (yellow-orange) was transferred under argon atmosphere into a 250 mL Fisher-Porter bottle charged with a frozen solution (-80 °C) of Ru(COD)(COT) (50 mg, 0.16 mmol, 0.5 equiv.) and Pt_2dba_3 (87.44 mg, 0.08 mmol of Pt_2dba_3, 0.5 equiv. of Pt) in 30 mL of THF (previously degassed). The Fischer-Porter reactor was pressurized with 3 bar of H_2, and the solution was stirred for 20 h at r.t. leading to a black homogeneous solution. After that, the remaining H_2 pressure was evacuated, the solution was concentrated to 2-3 mL, and 30 mL of pentane were added. The resulting black

precipitate was washed with pentane three times (50 mL) and dried overnight under vacuum. TGA gave the following metal content: 43 %. Yield: 50 mg, 42 %.

$RuPt_2$-dba: A Schlenk flask was charged with **PrIPr** (28.11 mg, 0.08 mmol, 0.17 equiv.) and KO*t*Bu (9.87 mg, 0.088 mmol). The solids were suspended in THF (30 mL) and stirred at r.t. for 20 h. The resulting solution (yellow-orange) was transferred under argon atmosphere into a 250 mL Fisher-Porter bottle charged with a frozen solution (-80 °C) of Ru(COD)(COT) (50 mg, 0.16 mmol, 0.33 equiv.) and Pt_2dba_3 (174.9 mg, 0.16 mmol of Pt_2dba_3, 0.66 equiv. of Pt) in 30 mL of THF (previously degassed). The Fischer-Porter reactor was pressurized with 3 bar of H_2, and the solution was stirred for 20 h at r.t leading to a black homogeneous solution. After that, the remaining H_2 pressure was evacuated, the solution was concentrated to 2-3 mL, and 30 mL of pentane were added. The resulting black precipitate was washed with pentane three times (50 mL) and dried overnight under vacuum. TGA gave the following metal content: 47 %. Yield: 110 mg, 67 %.

S2. HRTEM and SEM-EDX

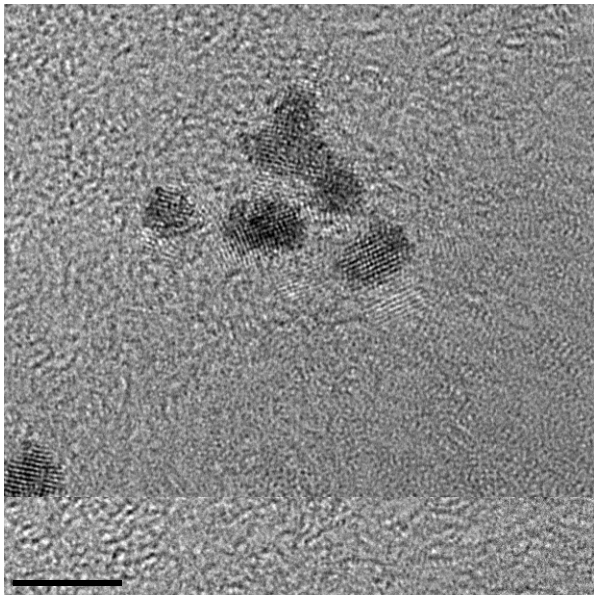

Figure S1. HRTEM micrograph of **RuPt-nor**

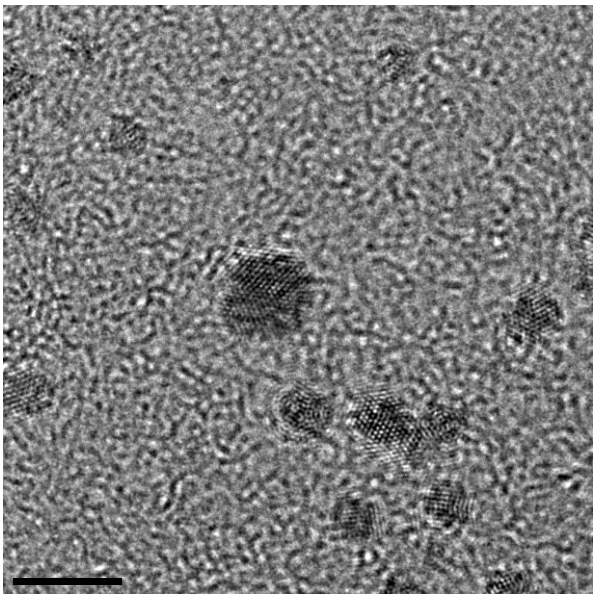

Figure S2. HRTEM micrograph of **RuPt-DMC**

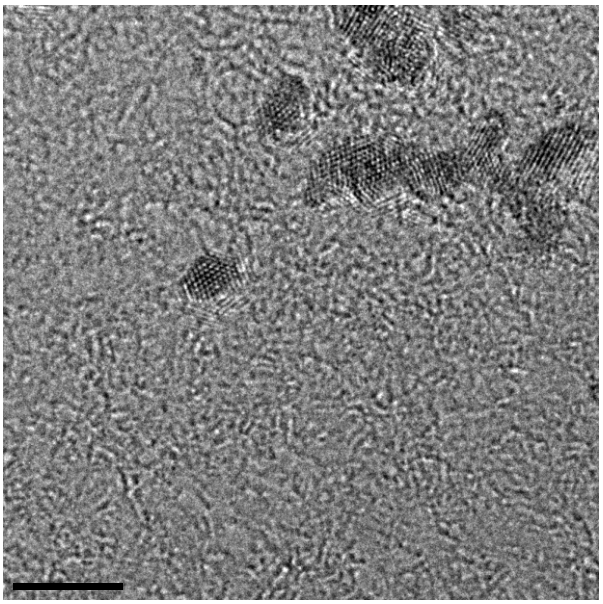

Figure S3. HRTEM micrograph of **$RuPt_2$-dba**

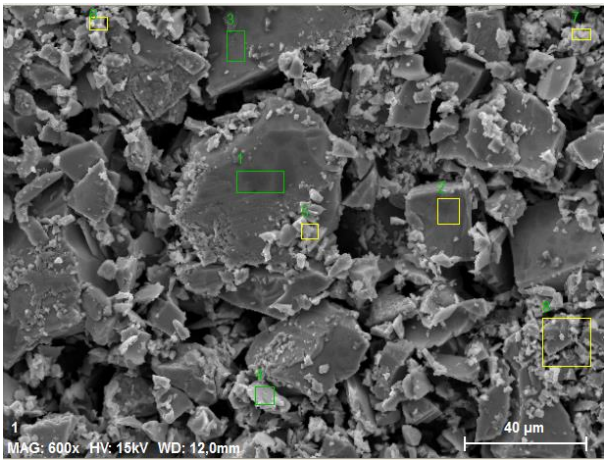

Element	Atom C [at.%]
Pt	4.06
C	50.42
Ru	4.22
O	26.54
K	4.06
N	8.91
S	1.78
	Total: 100

Figure S4. SEM-EDX analysis of **RuPt-nor**

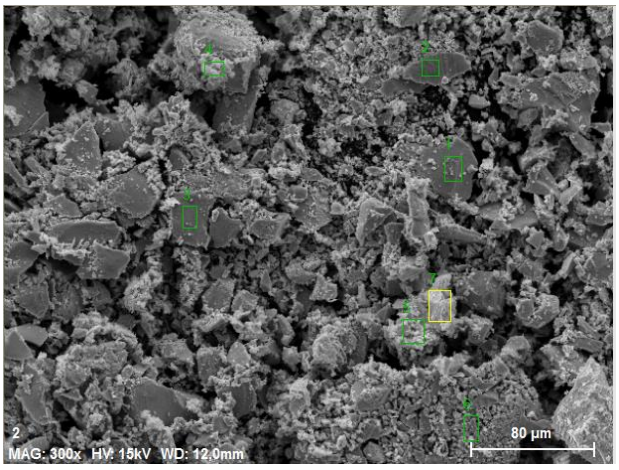

Element	Atom C [at.%]
Pt	5.76
C	62.74
Ru	5.95
O	19.58
K	3.41
N	8.91
S	2.56
	Total: 100

Figure S5. SEM-EDX analysis of **RuPt-DMC**

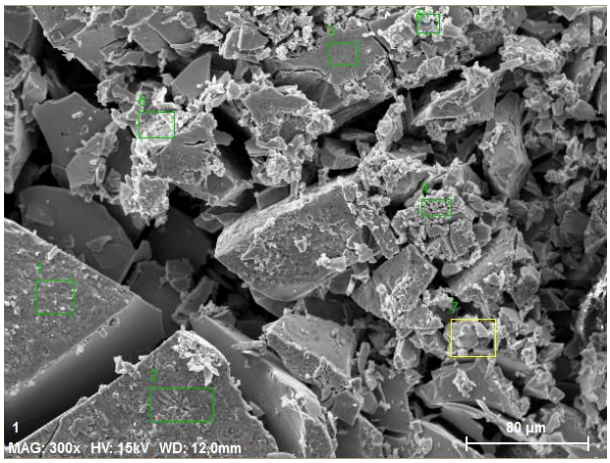

Element	Atom C [at.%]
Pt	4.50
C	54.92
Ru	4.20
O	30.12
K	4.34
N	8.91
S	1.59
	Total: 100

Figure S6. SEM-EDX analysis of **RuPt-DBA**

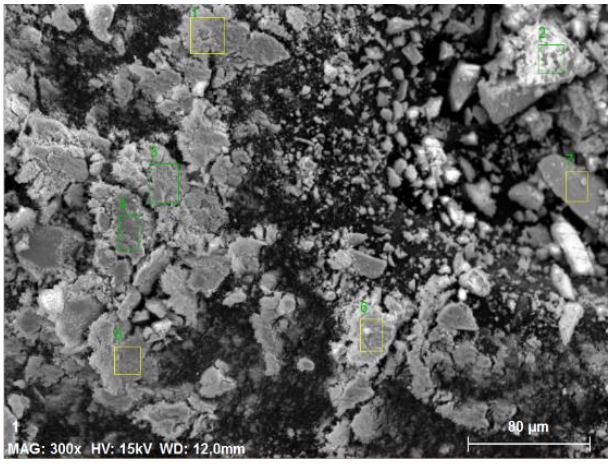

Element	Atom C [at.%]
Pt	4.65
C	60.76
Ru	2.20
O	20.44
K	3.76
N	7.17
S	1.03
	Total: 100

Figure S7. SEM-EDX analysis of **$RuPt_2$-DBA**

S3. WAXS

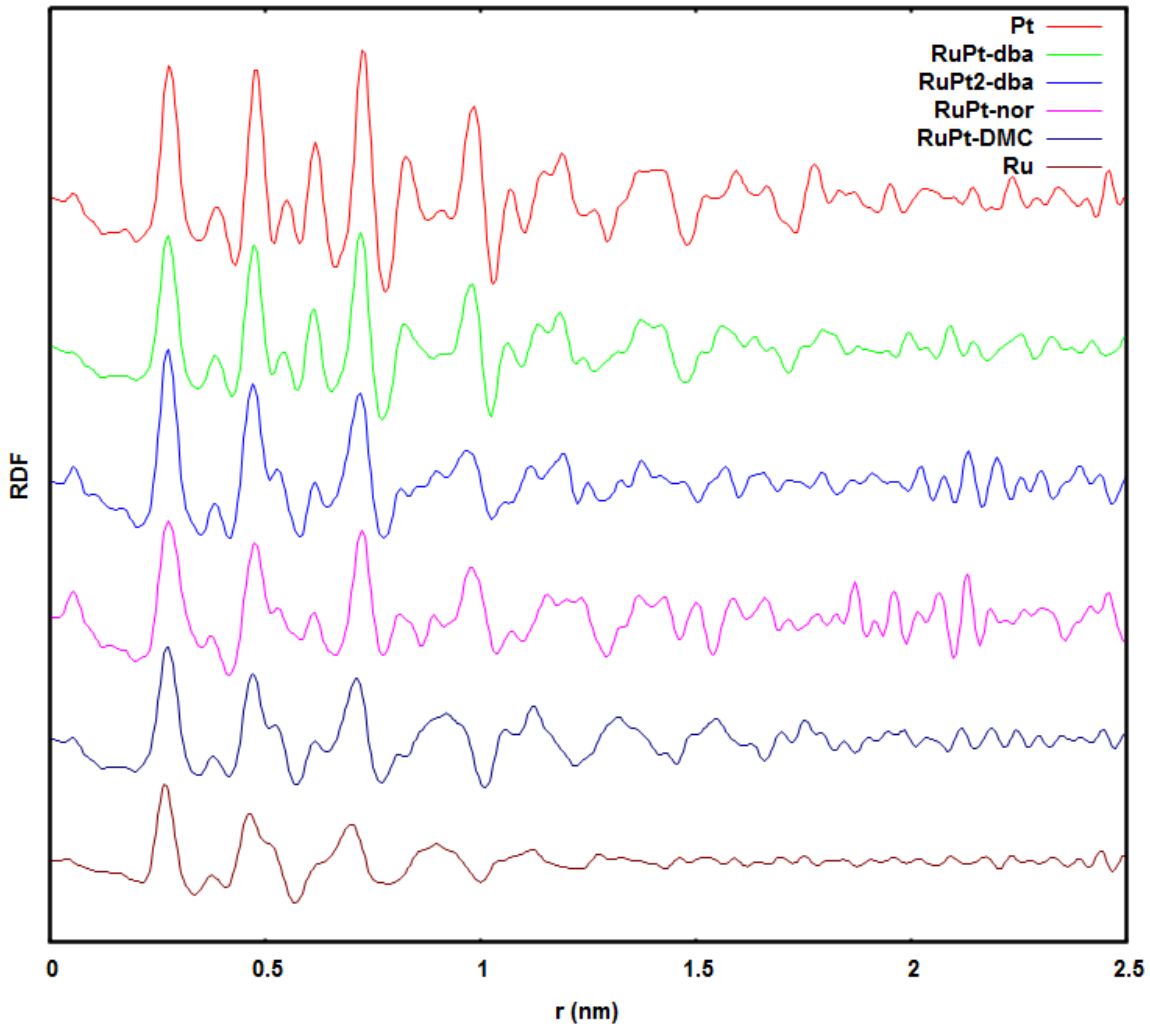

Figure S8. WAXS analysis of **Pt** (red), **RuPt-dba** (green), **RuPt$_2$-dba** (blue), **RuPt-nor** (pink), **RuPt-DMC** (dark blue), and **Ru** (brown). The RDF reflects metallic particles with structures evolving gradually from fcc for Pt to hcp for Ru (see 0.6-1.0 nm characteristic range).

S4. FT-IR

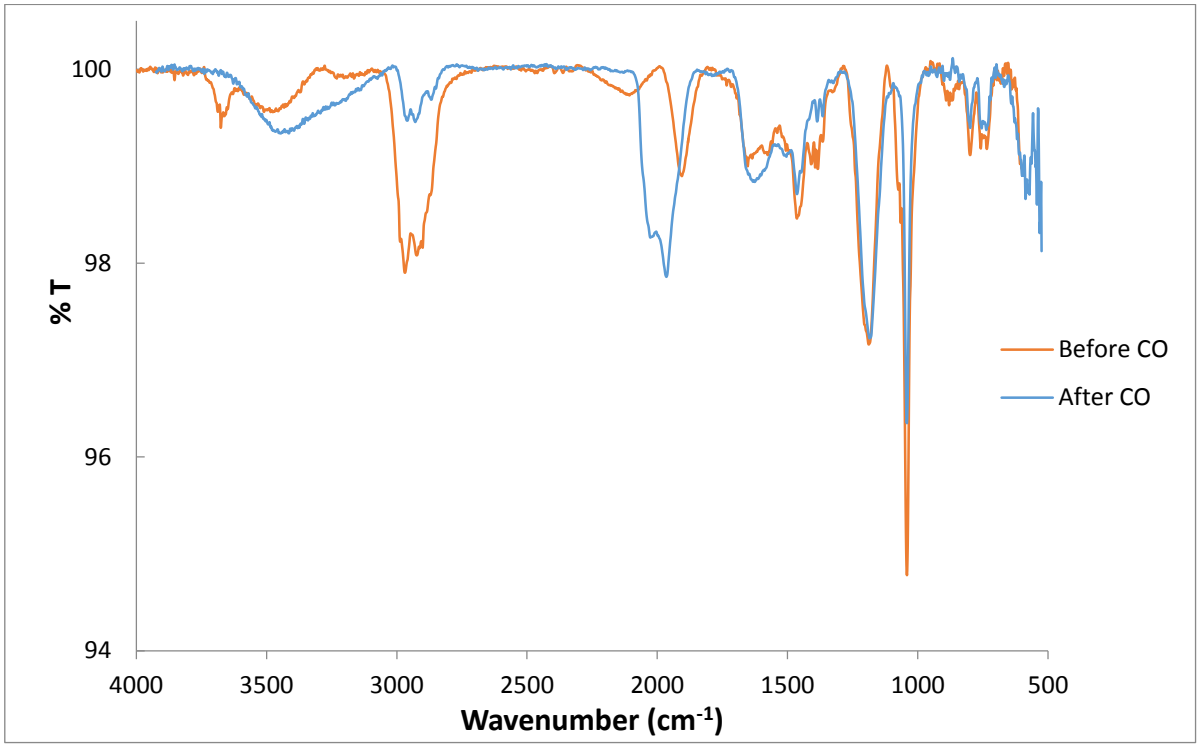

Figure S9. ATR FT-IR spectra of **Ru** NPs before (orange)*and after (blue) reaction with CO. The spectrum after exposure to CO exhibits the absorption bands of COt (1965 cm^{-1}) and *n*COt (2021 cm^{-1}).

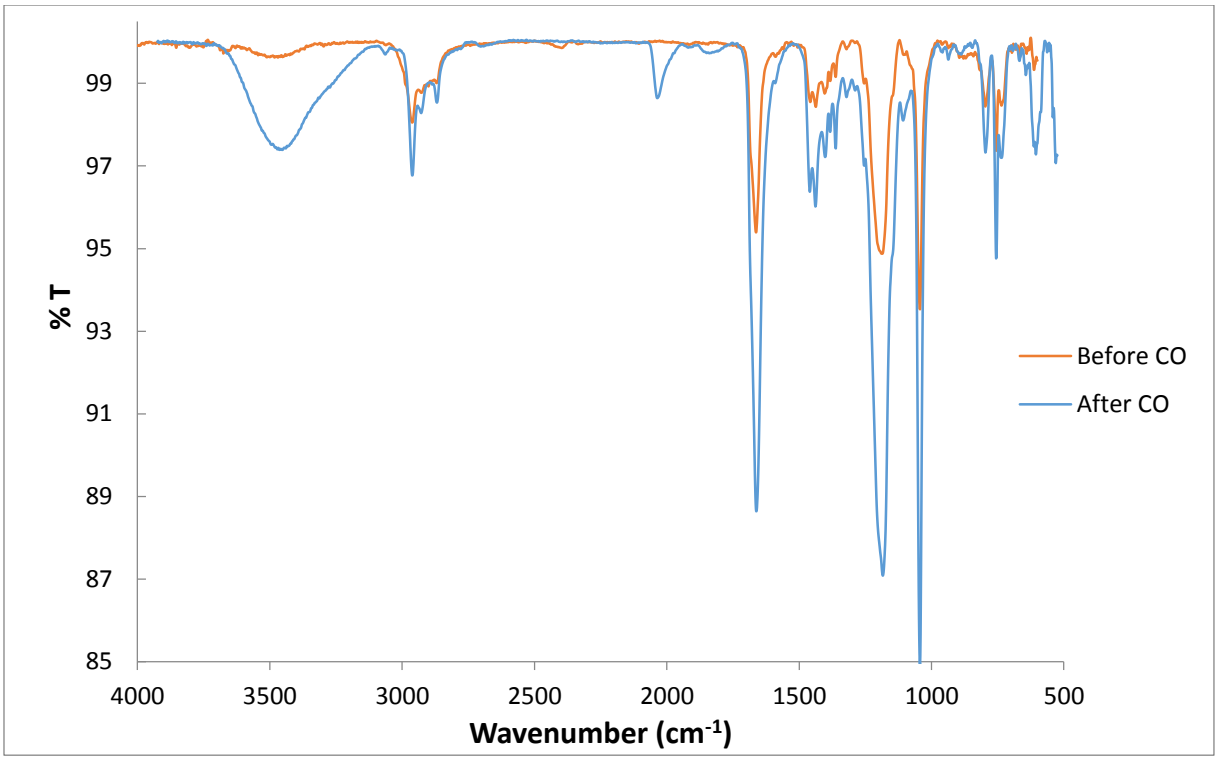

Figure S10. ATR FT-IR spectra of **Pt** NPs before (orange) and after (blue) reaction with CO. The spectrum after exposure to CO exhibits the characteristic absorption bands of COb (1830 cm^{-1}) and COt (2034 cm^{-1})

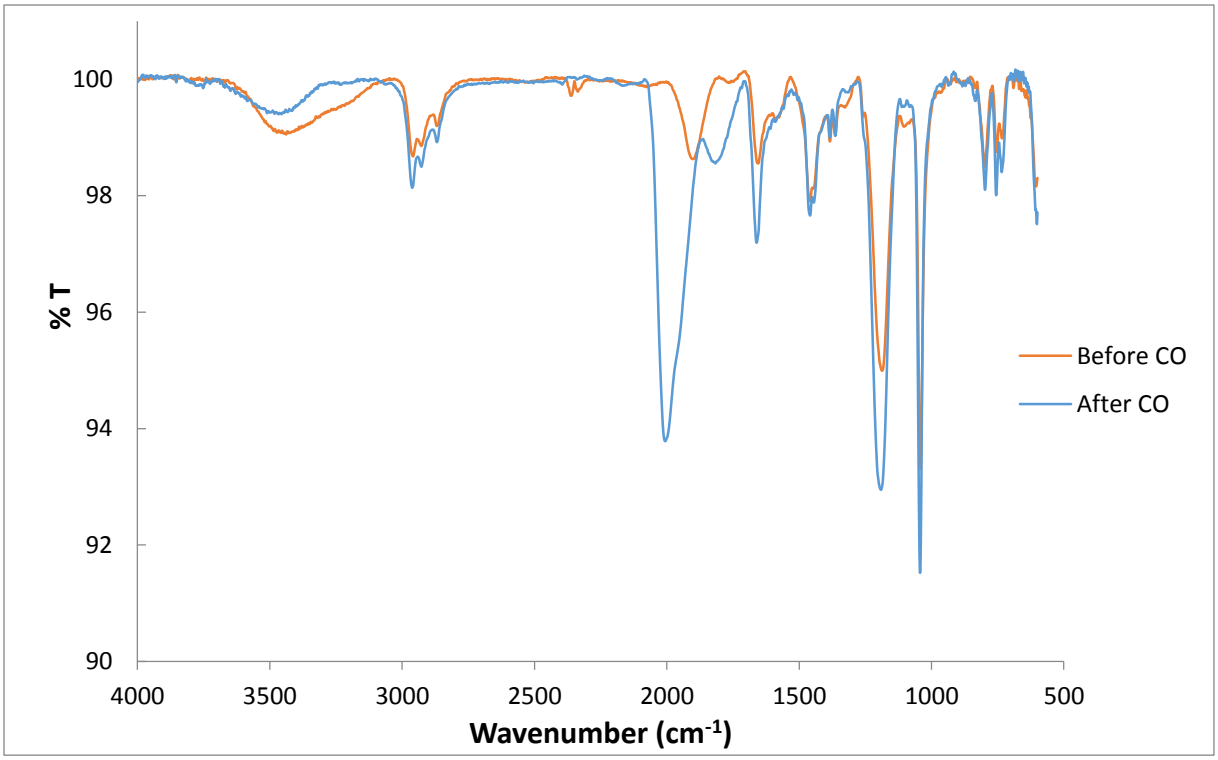

Figure S11. ATR FT-IR spectra of **RuPt-nor** NPs before (orange)* and after (blue) reaction with CO. The spectrum after exposure to CO exhibits the absorption bands of COb (1814 cm^{-1}) and COt (2003 cm^{-1}).

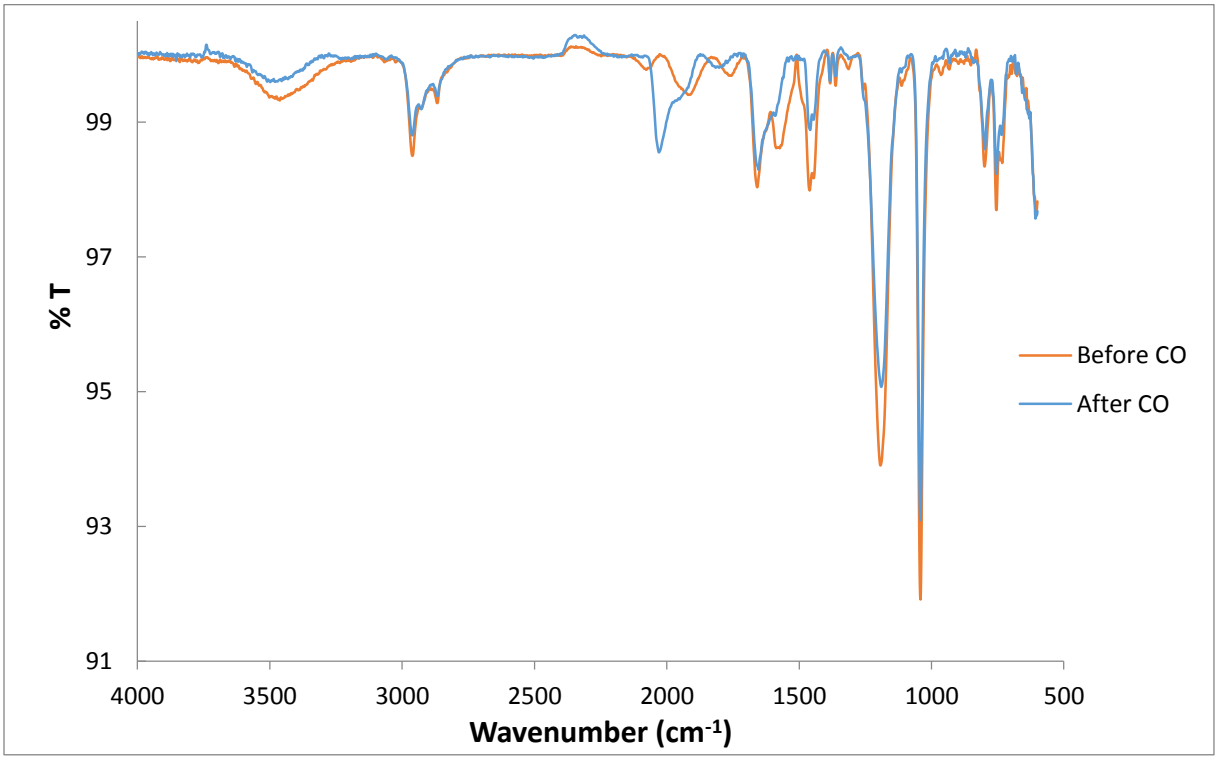

Figure S12. ATR FT-IR spectra of **RuPt-DMC** NPs before (orange)* and after (blue) reaction with CO. The spectrum after exposure to CO exhibits the absorption bands of COb (1814 cm^{-1}) and COt (2026 cm^{-1}).

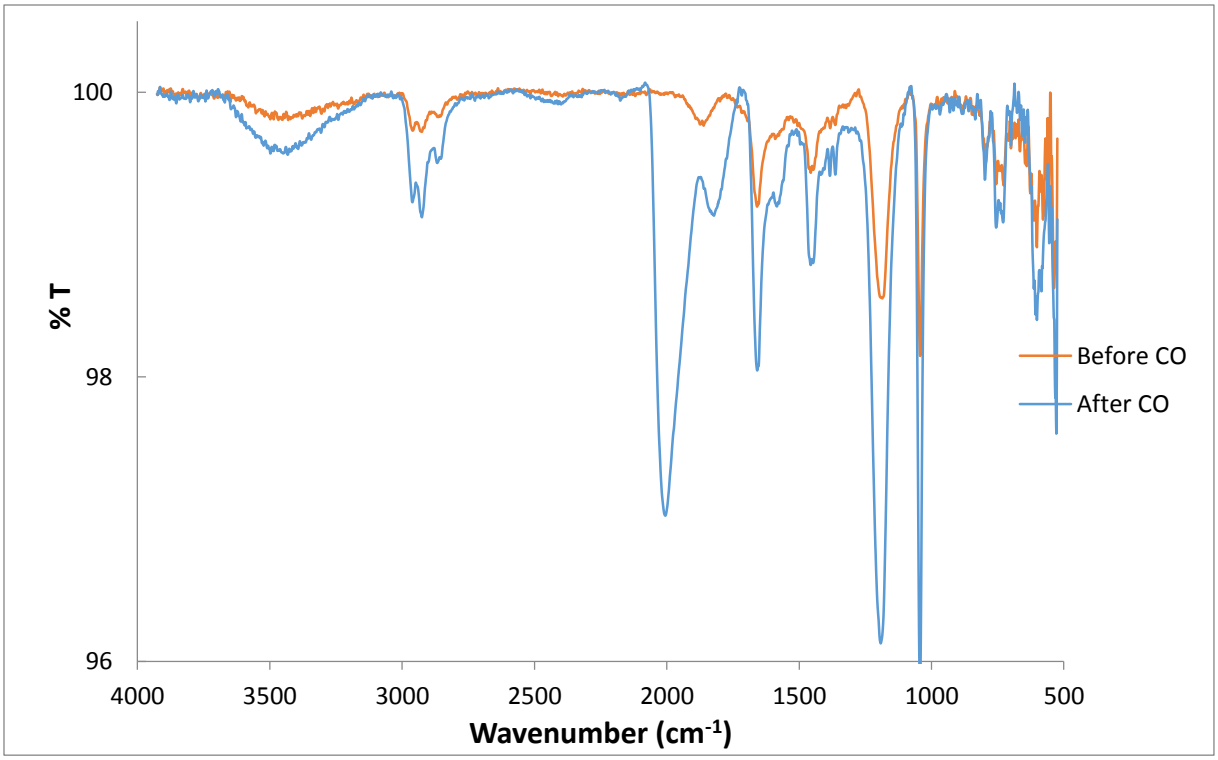

Figure S13. ATR FT-IR spectra of **RuPt-dba** NPs before (orange)* and after (blue) reaction with CO. The spectrum after exposure to CO exhibits the absorption bands of COb (1816 cm^{-1}) and COt (2005 cm^{-1}).

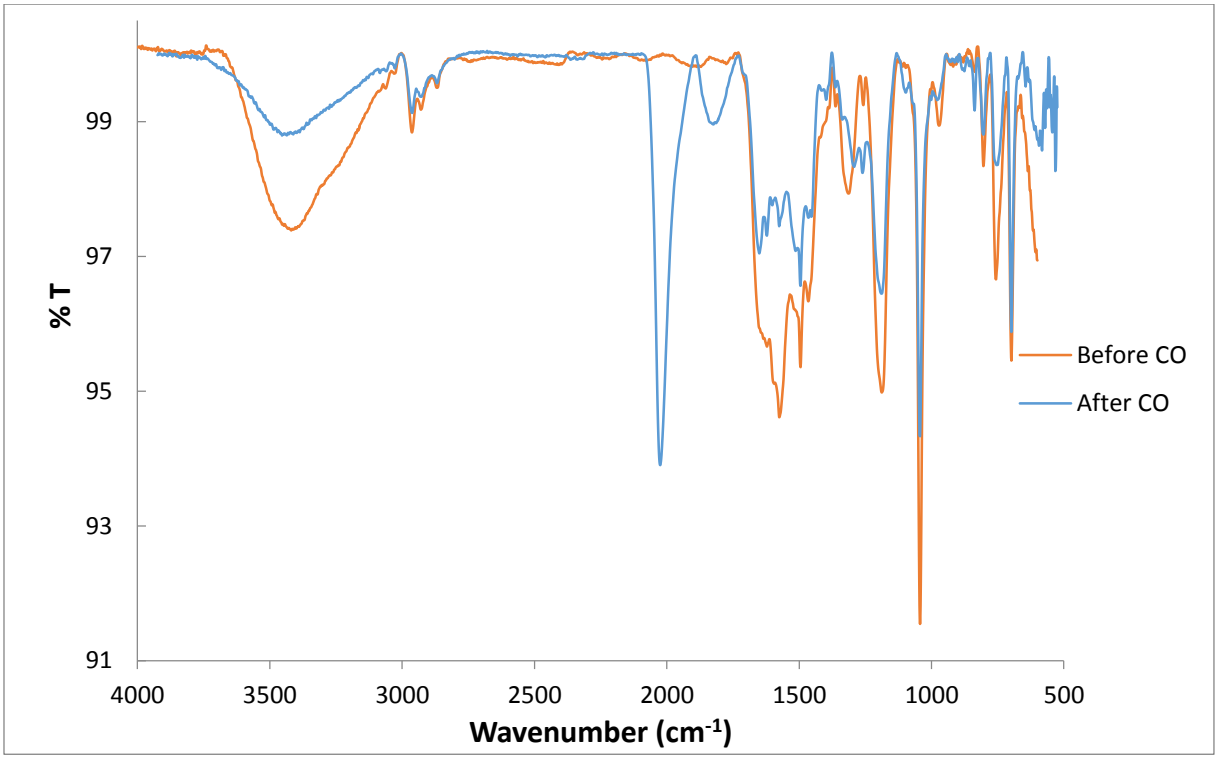

Figure S14. ATR FT-IR spectra of **$RuPt_2$-dba** NPs before (orange) and after (blue) reaction with CO. The spectrum after exposure to CO exhibits the absorption bands of COb (1824 cm^{-1}) and COt (2024 cm^{-1}).

* FT-IR spectra before (orange) exposure to carbon monoxide show a CO absorption band (1916-1922 cm^{-1}) in Figures S11, S12, S12 and S14. This CO was produced during the Ru NPs synthesis through a decarbonylation process of the THF used as solvent.[2]

[2] L. M. Martínez-Prieto, C. Urbaneja, P. Palma, J. Campora, K. Philippot, B. Chaudret, *Chem. Comm.* **2015**, *51*, 4647.

S5. MAS NMR

Before ^{13}CO exposure:

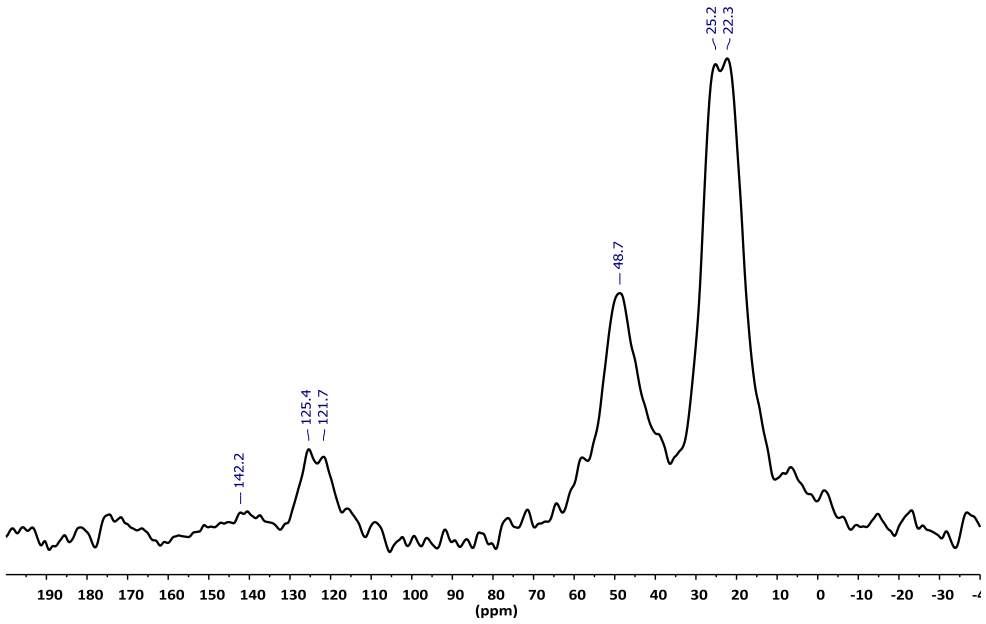

Figure S15. ^{13}C CP-MAS NMR spectrum of **Ru** NPs. Signals: 142.2 ppm quaternary carbons of aromatic ring; ~ 125-121 ppm protonated carbons of aromatic ring and imidazolium backbone; 48.7 ppm α and γ alkyl chain CH_2 groups of the sulfonated N-substituent; ~ 26-22 ppm isopropyl and β alkyl chain CH_2 groups. The imidazolium carbene carbon is not observed due to a broadening of the peak.

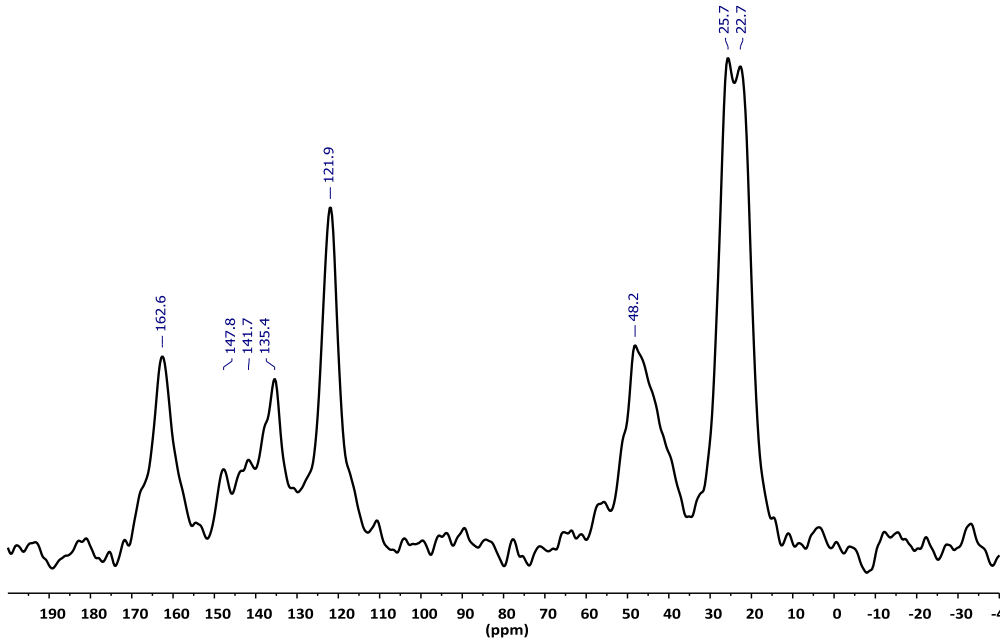

Figure S16. ^{13}C CP-MAS NMR spectrum of **Pt** NPs. Signals: 162.6 ppm imidazolium carbene carbon; ~ 148-135 ppm quaternary carbons of aromatic ring; 121.9 ppm protonated carbons of aromatic ring and imidazolium backbone; 48.2 ppm α and γ alkyl chain CH_2 groups of the sulfonated N-substituent; ~ 26-22 ppm isopropyl and β alkyl chain CH_2 groups.

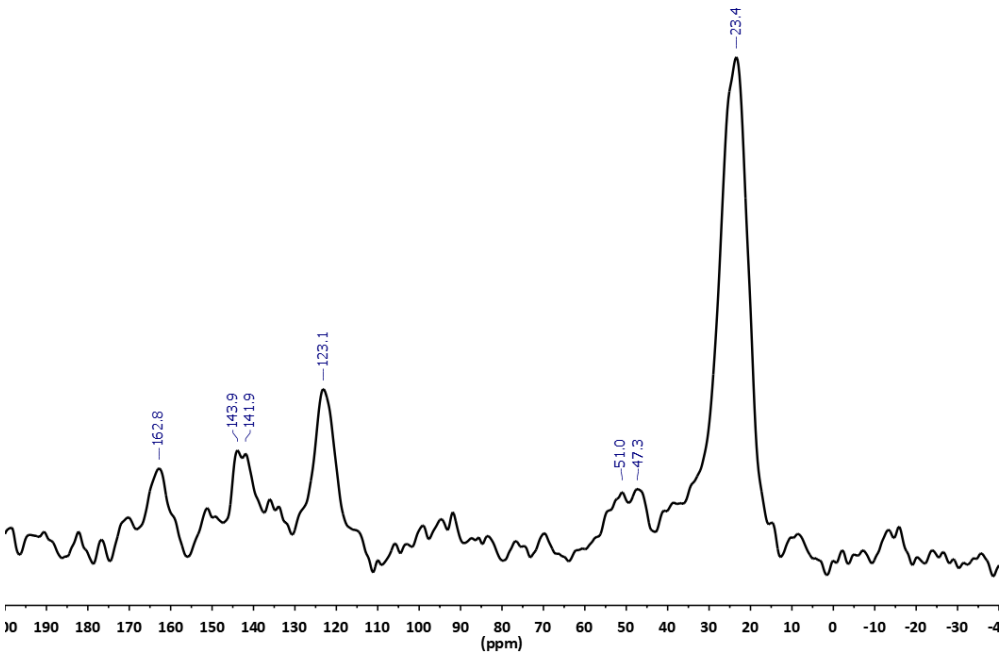

Figure S17. ^{13}C CP-MAS NMR spectrum of **RuPt-nor** NPs. Signals: 162.8 ppm imidazolium carbene carbon; ~143-141 ppm quaternary carbons of aromatic ring; 123.1 ppm protonated carbons of aromatic ring and imidazolium backbone; ~51-47 ppm α and γ alkyl chain CH_2 groups of the sulfonated N-substituent; 23.4 ppm isopropyl and β alkyl chain CH_2 groups.

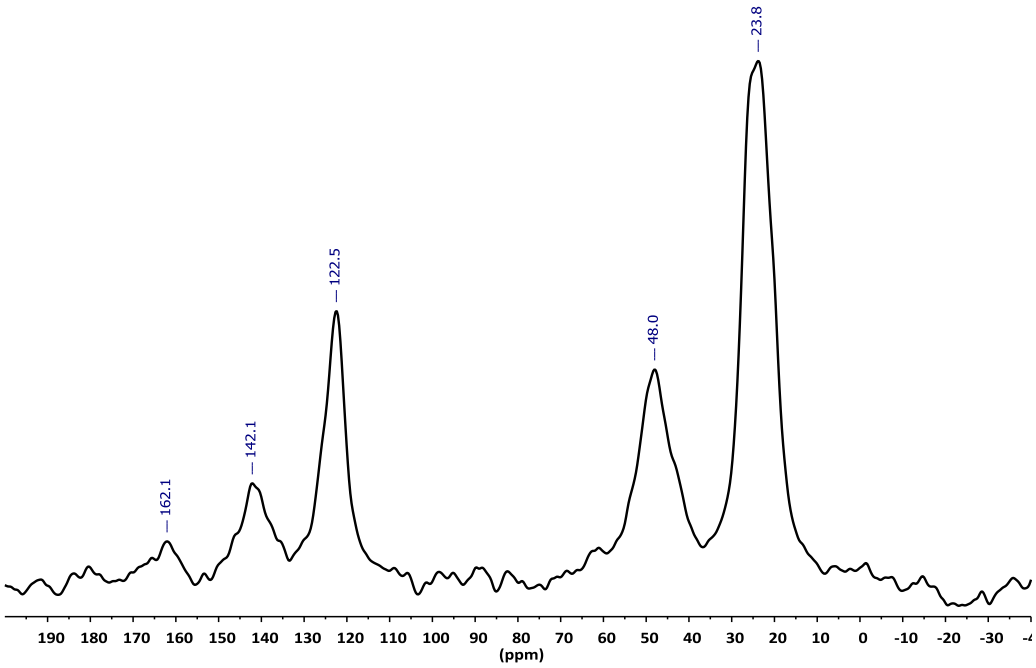

Figure S18. ^{13}C CP-MAS NMR spectrum of **RuPt-DMC** NPs. Signals: 162.1 ppm imidazolium carbene carbon; 142.1 ppm quaternary carbons of aromatic ring; 122.5 ppm protonated carbons of aromatic ring and imidazolium backbone; 48 ppm α and γ alkyl chain CH_2 groups of the sulfonated N-substituent; 23.8 ppm isopropyl and β alkyl chain CH_2 groups.

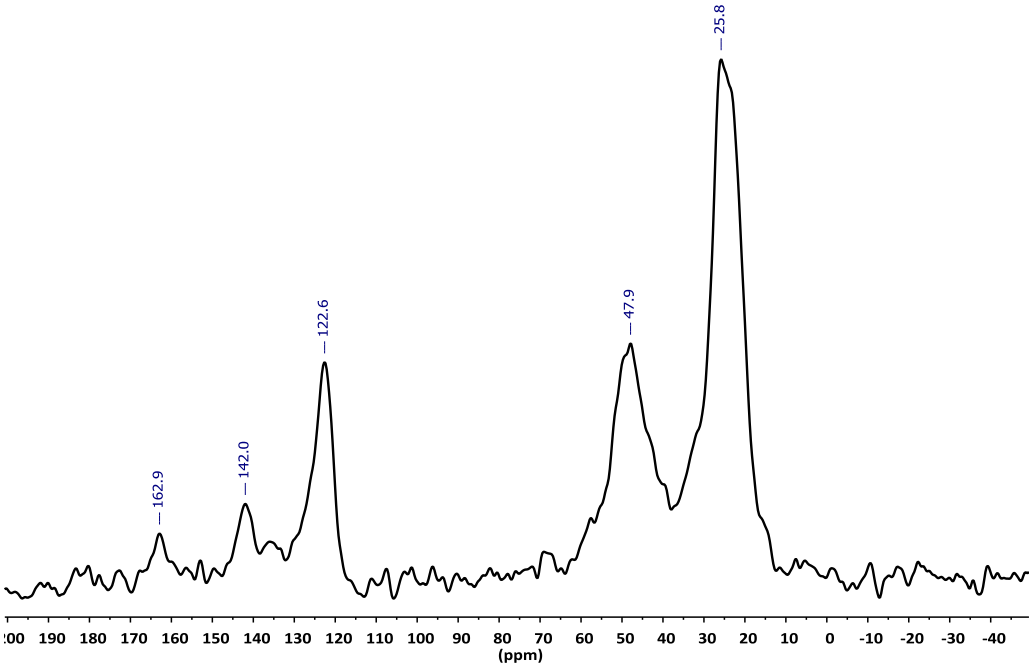

Figure S19. ^{13}C CP-MAS NMR spectrum of **RuPt-dba** NPs. Signals: 162.9 ppm imidazolium carbene carbon; 142.0 ppm quaternary carbons of aromatic ring; 122.6 ppm protonated carbons of aromatic ring and imidazolium backbone; 47.9 ppm α and γ alkyl chain CH_2 groups of the sulfonated N-substituent; 25.8 ppm isopropyl and β alkyl chain CH_2 groups.

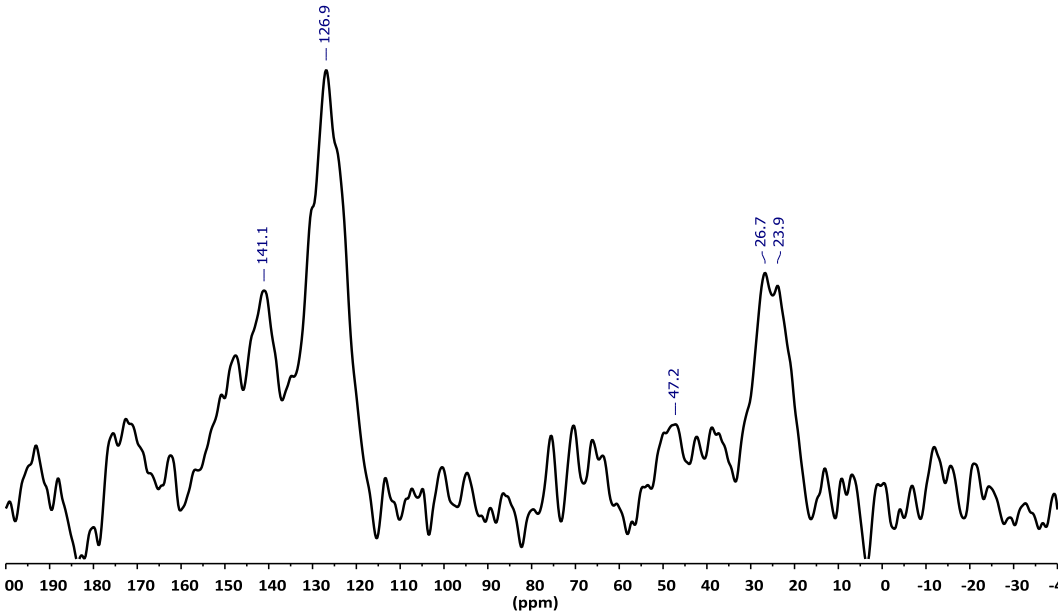

Figure S20. ^{13}C CP-MAS NMR spectrum of **$RuPt_2$-dba** NPs. Signals: 141.1 ppm quaternary carbons of aromatic ring; 126.9 ppm protonated carbons of aromatic ring and imidazolium backbone; 47.2 ppm α and γ alkyl chain CH_2 groups of the sulfonated N-substituent; ~ 27-23 ppm isopropyl and β alkyl chain CH_2 groups. The imidazolium carbene carbon is not observed due to a broadening of the peak.

After ^{13}CO exposure:

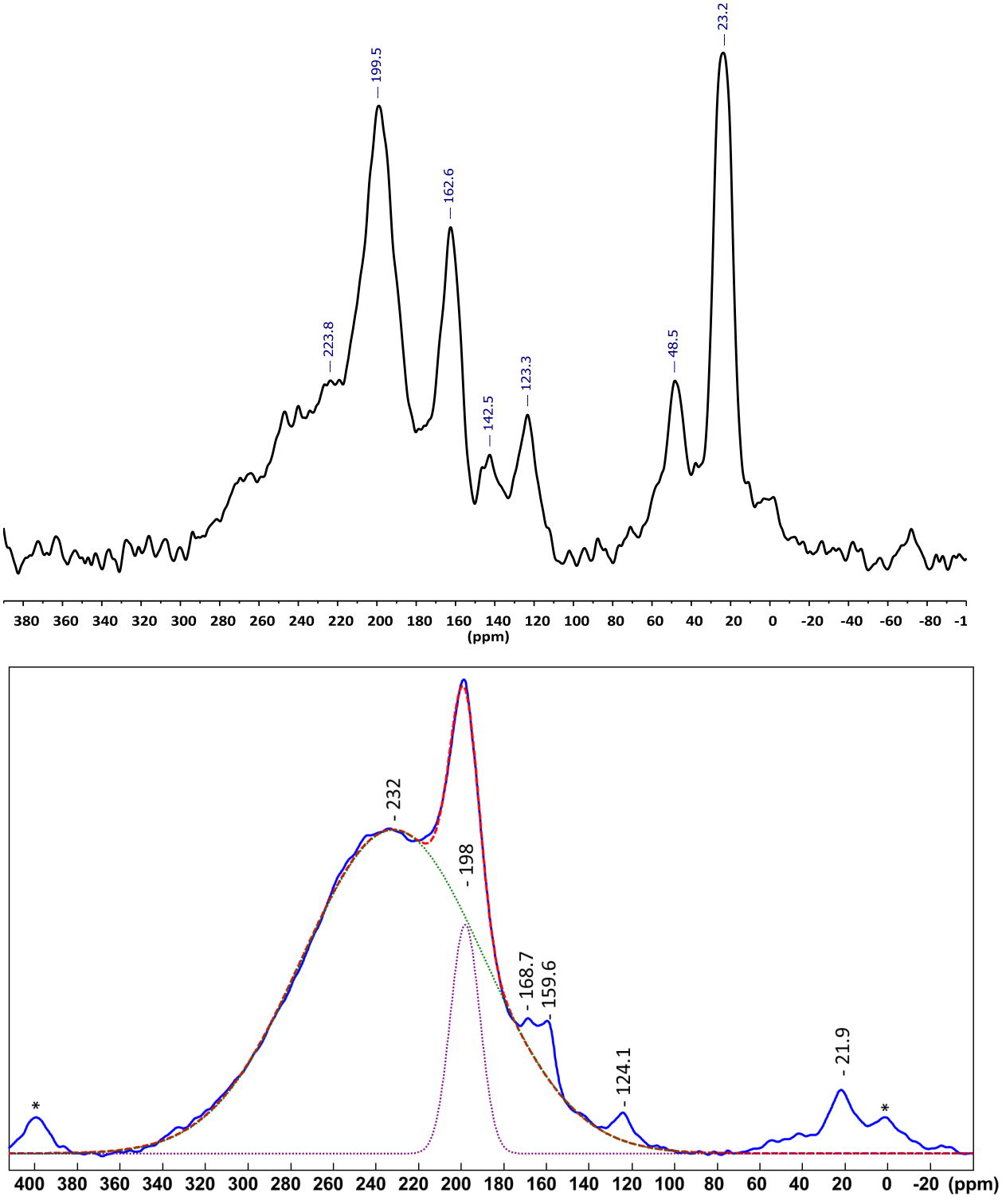

Figure S21. ^{13}C CP-MAS (top) and Hahn-echo (bottom) NMR spectra of **Ru** NPs after exposure to ^{13}CO (1 bar, 18 h, at r.t.). In red, deconvolution of the CO signals of the ^{13}C Hahn-echo NMR spectrum. * Spinning Sidebands of CO_t.

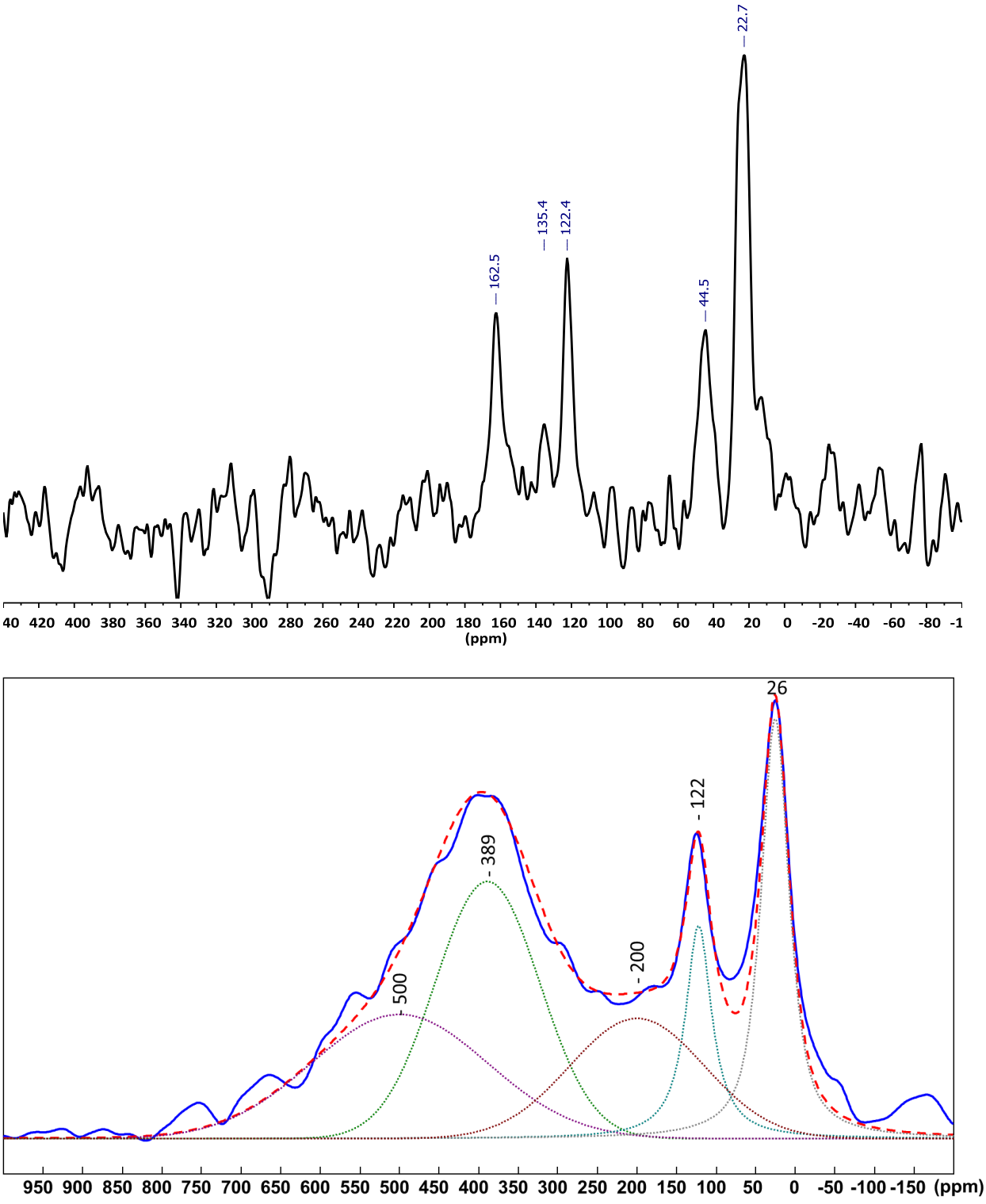

Figure S22. ^{13}C CP-MAS (top) and Hahn-echo (bottom) NMR spectra of **Pt** NPs after exposure to ^{13}CO (1 bar, 18 h, at r.t.). In red, signal deconvolution of the ^{13}C Hahn-echo NMR spectrum.

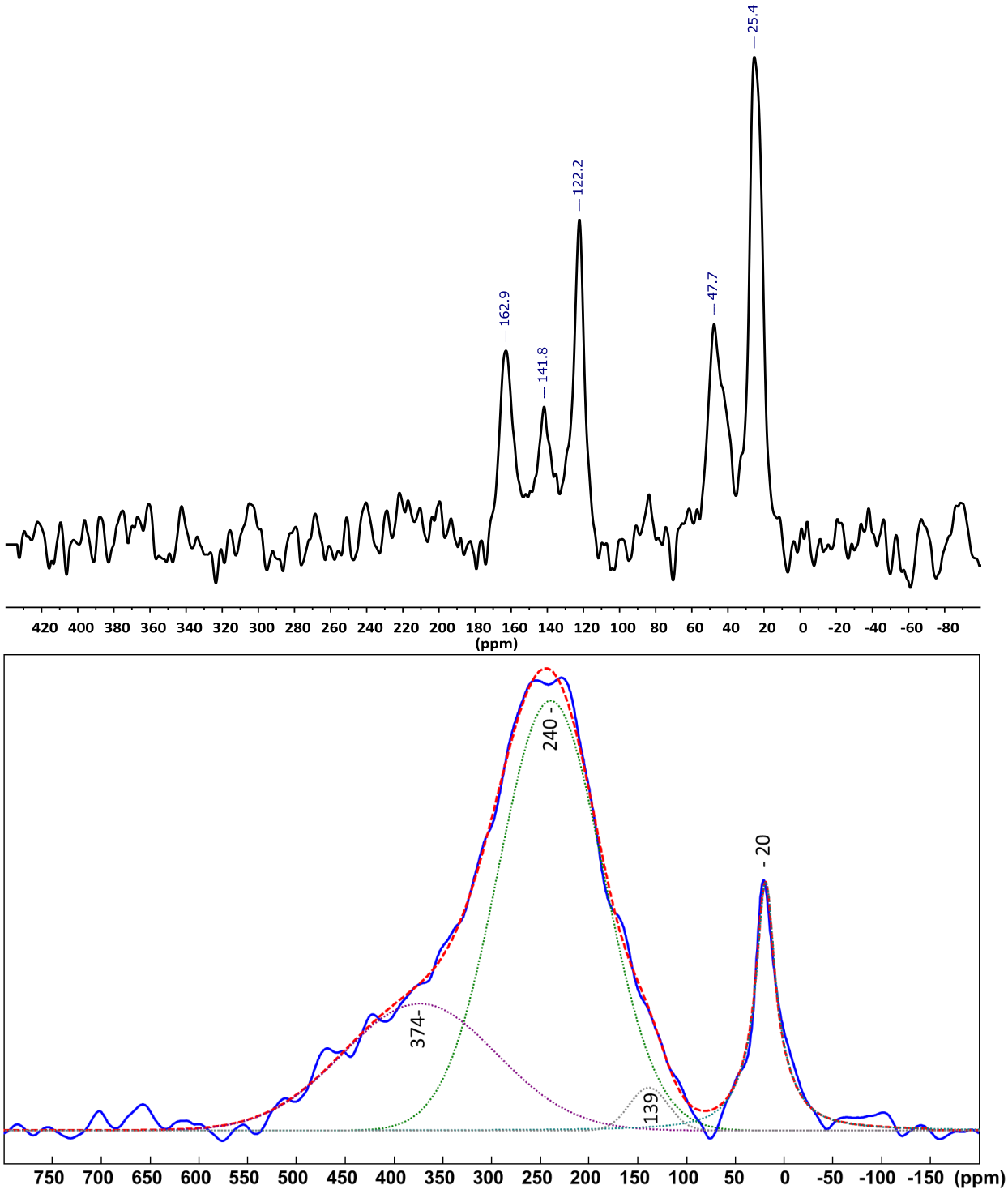

Figure S23. ^{13}C CP-MAS (top) and Hahn-echo (bottom) NMR spectra of **RuPt-nor** NPs after exposure to ^{13}CO (1 bar, 18 h, at r.t.). In red, signal deconvolution of the ^{13}C Hahn-echo NMR spectrum.

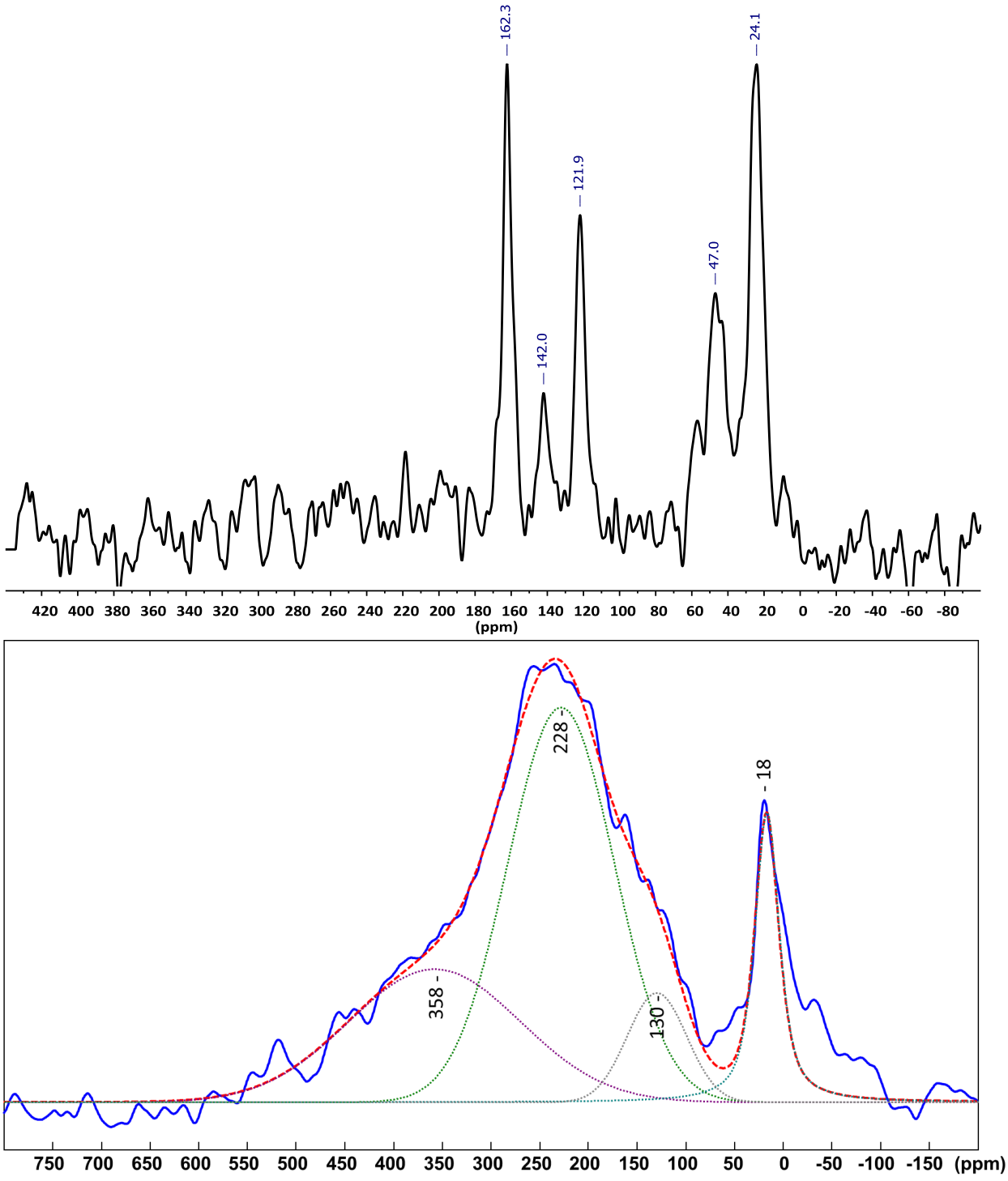

Figure S24. ^{13}C CP-MAS (top) and Hahn-echo (bottom) NMR spectra of **RuPt-DMC** NPs after exposure to ^{13}CO (1 bar, 18 h, at r.t.). In red, signal deconvolution of the ^{13}C Hahn-echo NMR spectrum.

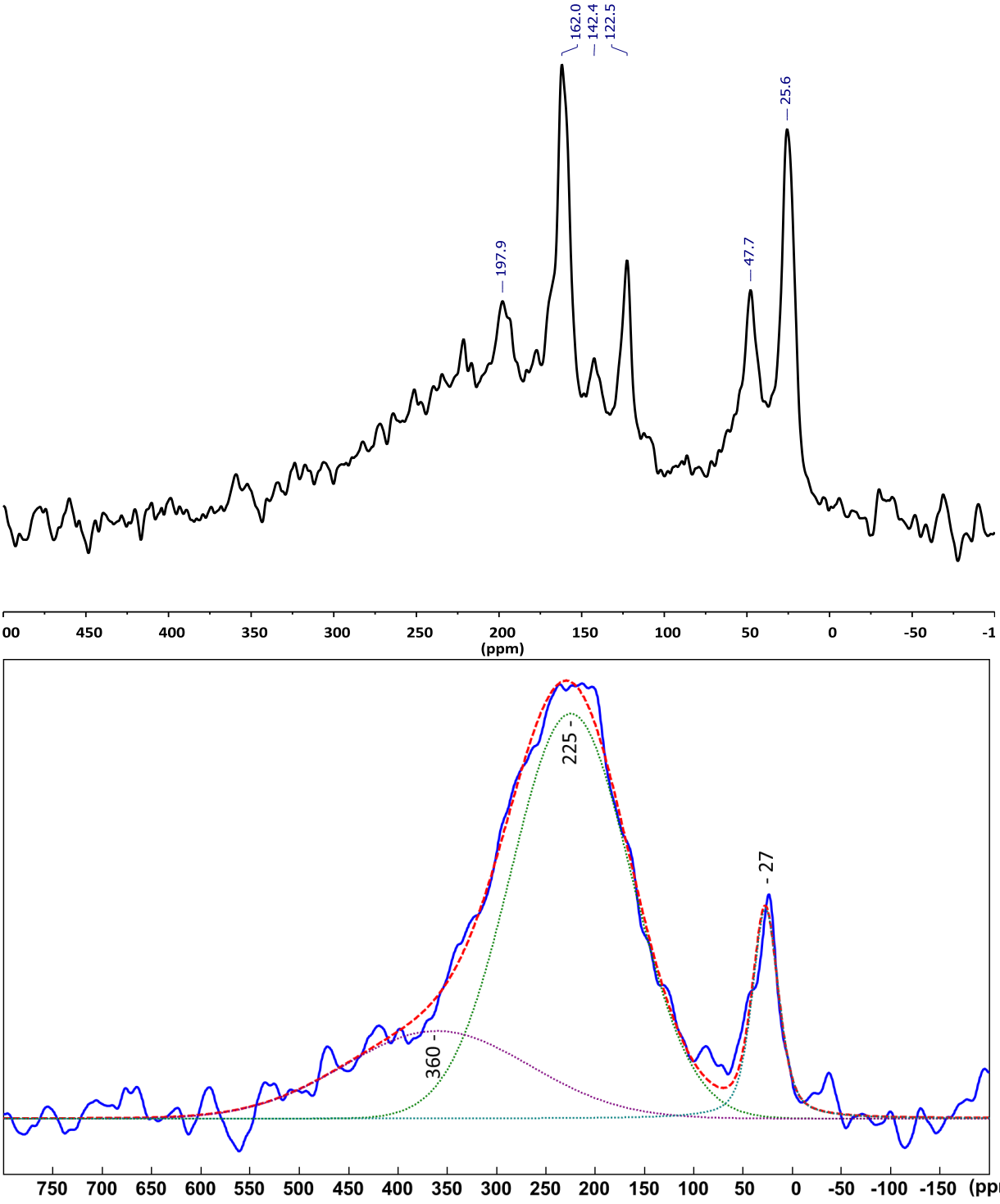

Figure S25. ^{13}C CP-MAS (top) and Hahn-echo (bottom) NMR spectra of **RuPt-dba** NPs after exposure to ^{13}CO (1 bar, 18 h, at r.t.). In red, signal deconvolution of the ^{13}C Hahn-echo NMR spectrum.

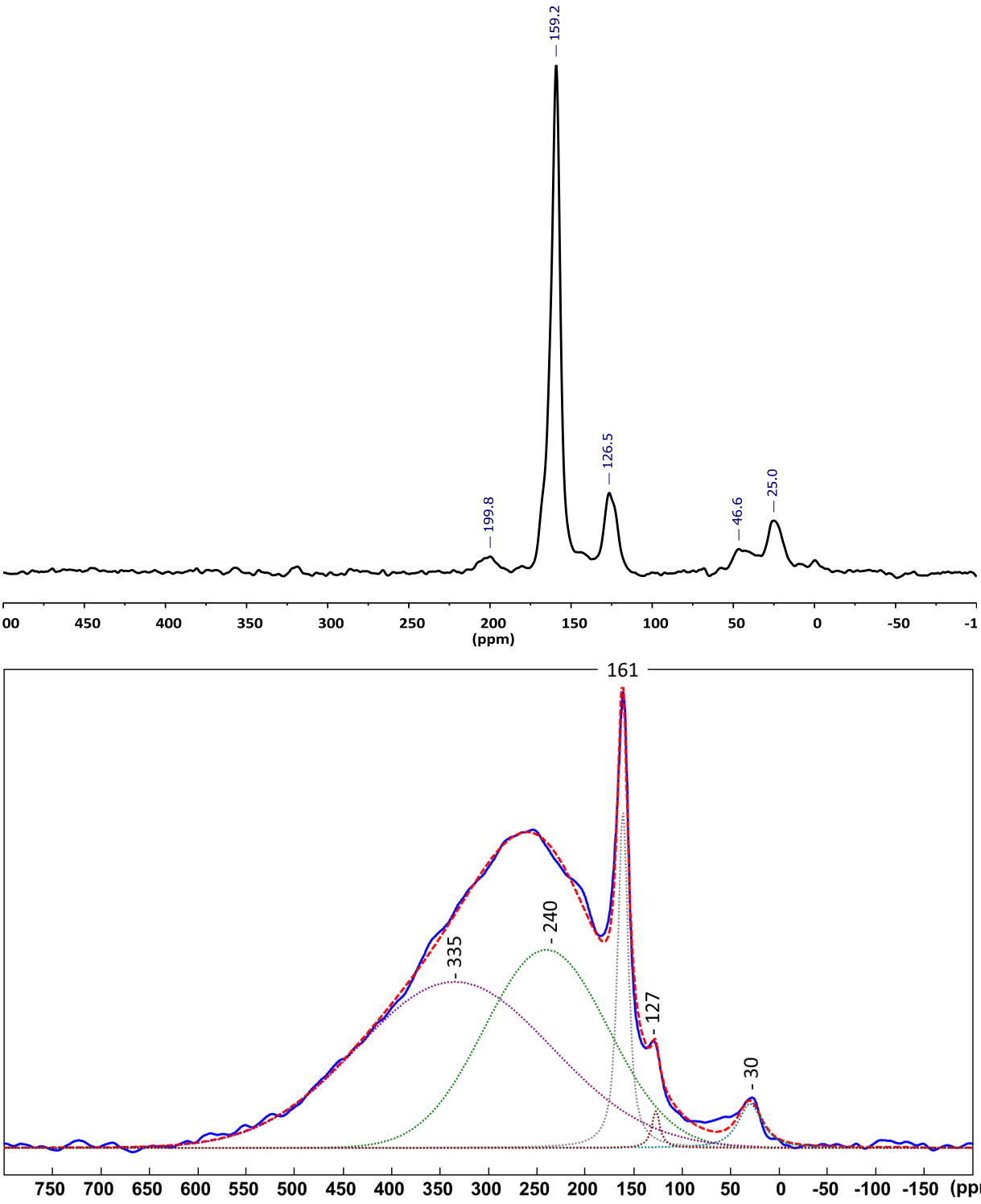

Figure S26. ^{13}C CP-MAS (top) and Hahn-echo (bottom) NMR spectra of **$RuPt_2$-dba** NPs after exposure to ^{13}CO (1 bar, 18 h, at r.t.). In red, signal deconvolution of the ^{13}C Hahn-echo NMR spectrum.

S7. Catalytic data

General procedure for deuteration reactions

A 90 mL Fisher-Porter reactor was charged with NPs (2-3 mg, 6-7 mol %) in a glove box under argon. A solution of L-lysine (21.92 mg, 0.15 mmol) in D_2O (2 mL) was added and the reaction mixture was stirred at 55 °C under 2 bar D_2 during 42 hours. The final product was analyzed directly through ^1H NMR. The H/D exchange percentage was determined by the decrease of integral intensities at the specified positions compared to the starting material. Integral intensities were calibrated against hydrogen signals of position β which do not undergo H/D-exchange.

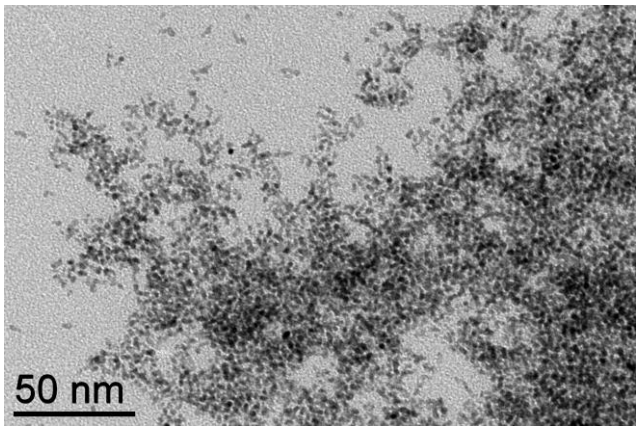

Figure S27. TEM pictures of RuPt-dba NPs after catalysis on L-lysine under 2 bars of D_2 for 42h (in comparison to Figure 1e before catalysis).

S8. Solution NMR

^{1}H NMR spectrum of Commercial L-lysine:

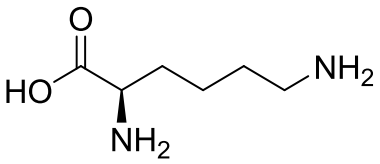

^{1}H NMR (400 MHz, D2O) δ 3.72 (t, *J* = 6.13 Hz, 1H), 2.96 - 3.02 (m, 2H), 1.82 - 1.92 (m, 2H), 1.69 (quin, *J* = 7.64 Hz, 2H), 1.34 - 1.53 (m, 2H).

^{1}H NMR spectra of L-lysine after deuteration with Ru NPs:

1. Ru NPs**:**

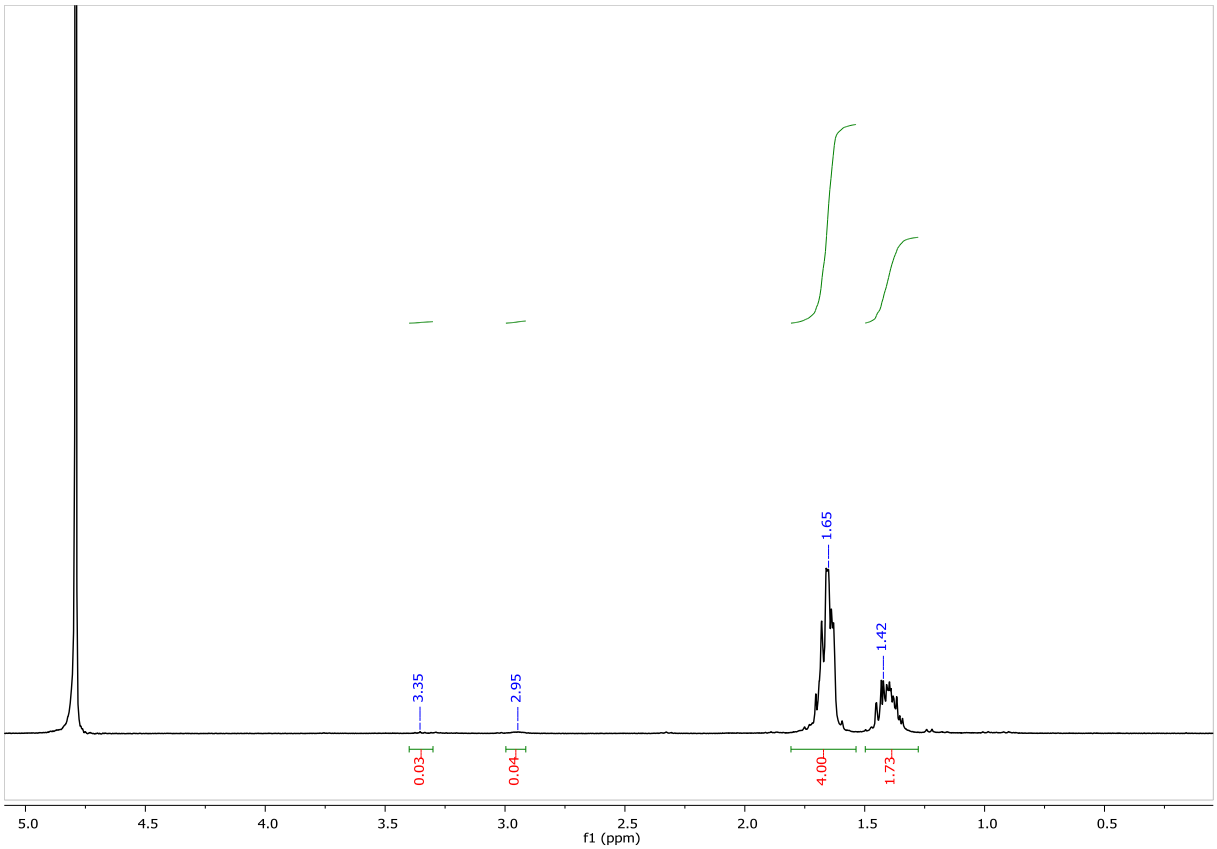

Figure S28. ^{1}H NMR spectrum after deuteration of L-lysine using Ru NPs as catalyst.

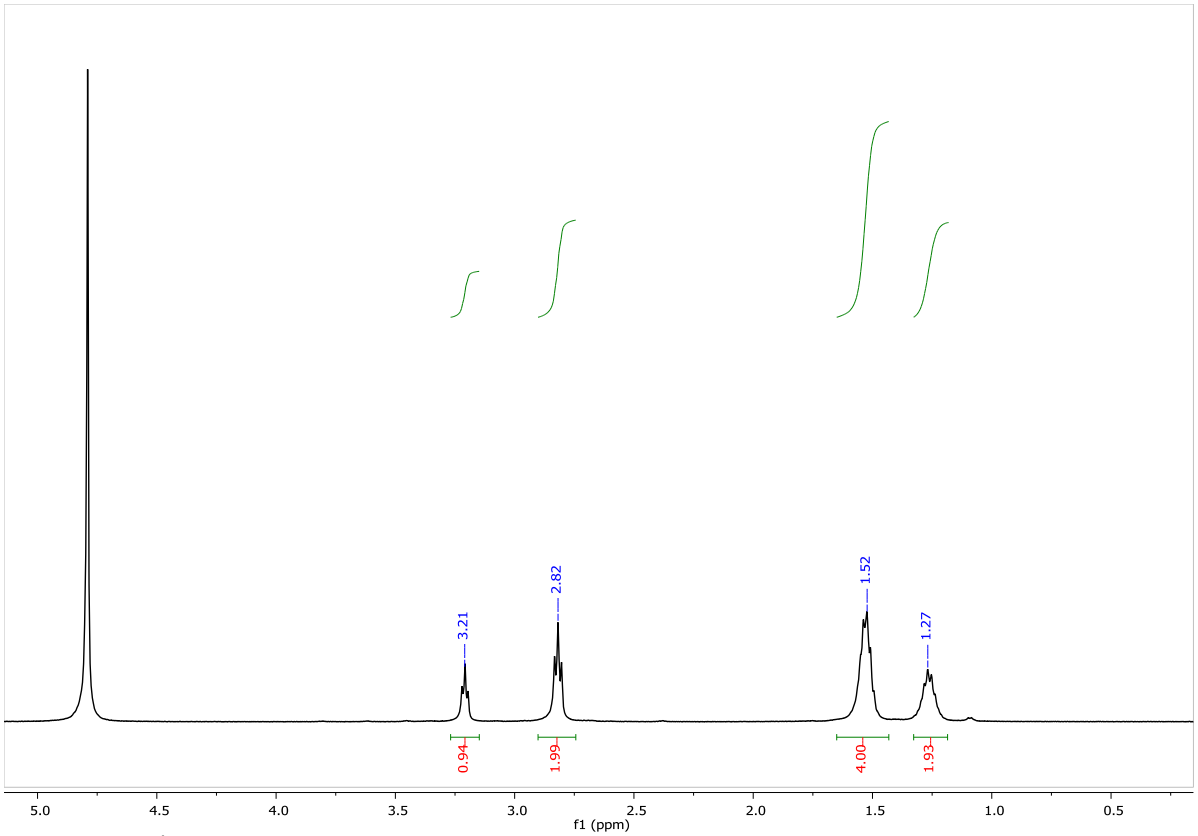

Figure S29. ^{1}H NMR spectrum after deuteration of L-lysine using Pt NPs as catalyst.

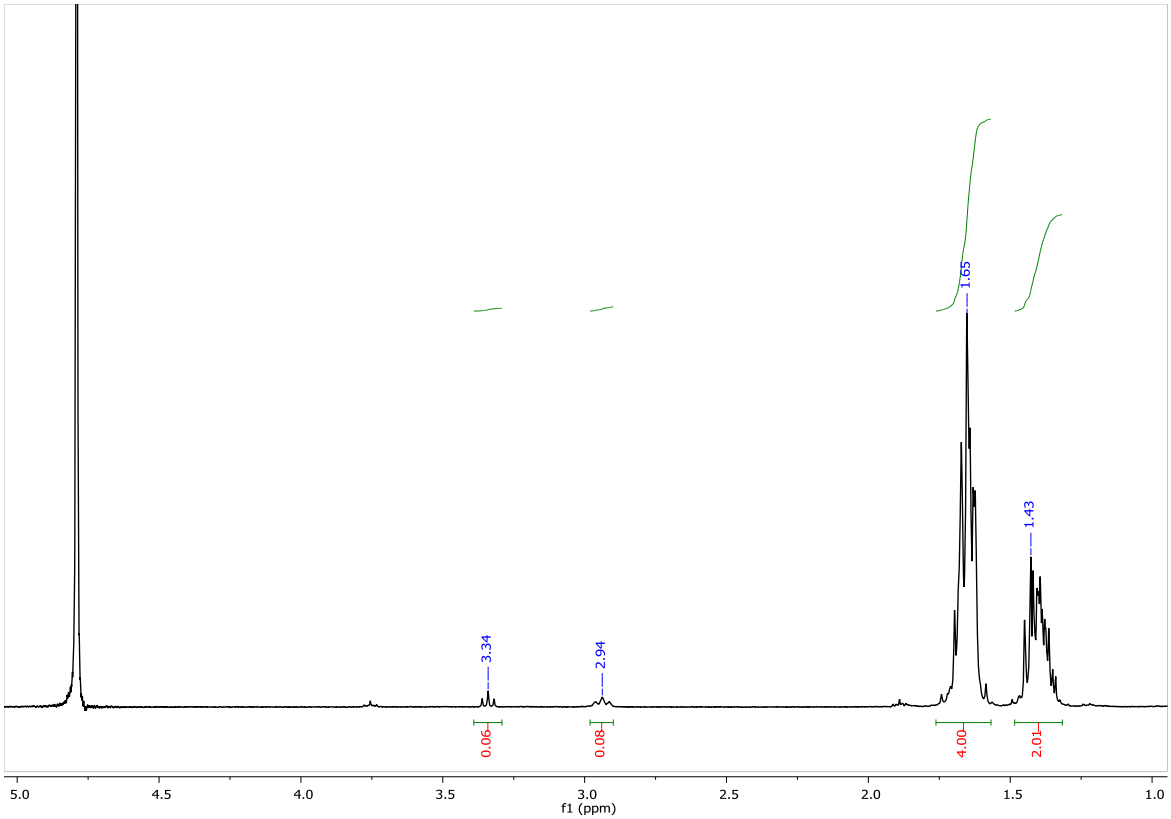

Figure S30. ^{1}H NMR spectrum after deuteration of L-lysine using RuPt-nor NPs as catalyst.

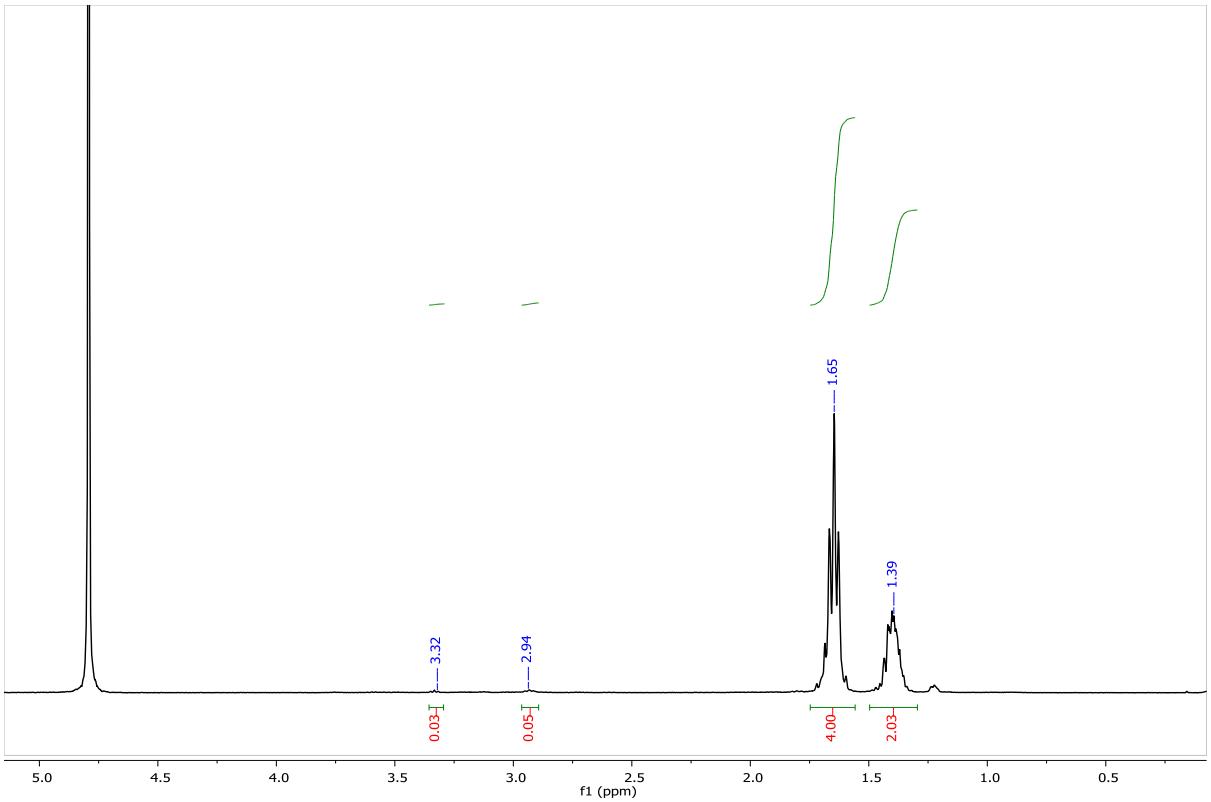

Figure S31. ^{1}H NMR spectrum after deuteration of L-lysine using RuPt-DMC NPs as catalyst.

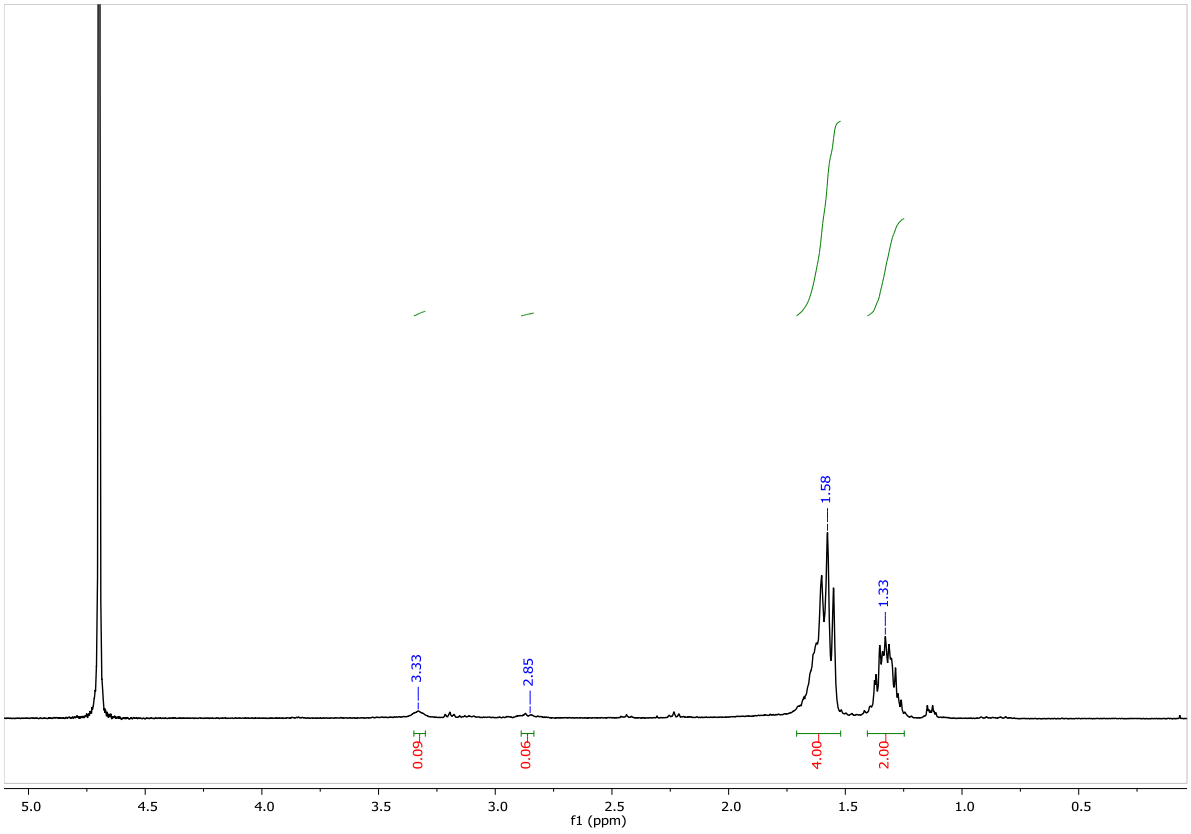

Figure S32. ^{1}H NMR spectrum after deuteration of L-lysine using RuPt-dba NPs as catalyst.

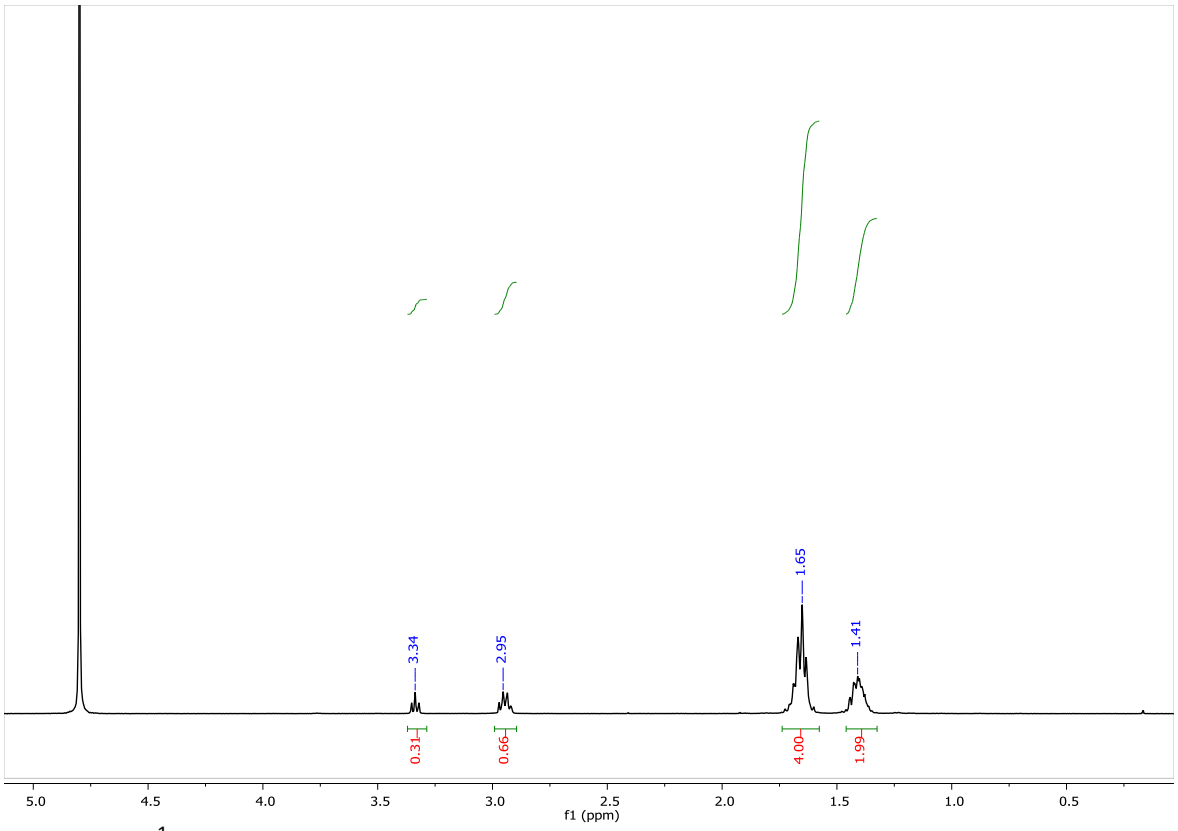

Figure S33. ^{1}H NMR spectrum after deuteration of L-lysine using $RuPt_2$-dba NPs as catalyst.

S9. Chemical shift perturbation

^{1}H, ^{13}C HSQC spectra of different amounts of L-lysine (2, 5, 10 and 20mg in 600µL of D_2O) with 1 mg/mL of NPs were recorded. Spectra were recorded at natural abundance on an 800MHz Bruker NMR spectrometer, equipped with a QCP cryogenic probehead. We used a sensitivity enhanced HSQC sequence[3] with 2048 × 256 points for the ^{1}H respectively ^{13}C dimension, corresponding to a spectral window of 13.9486 × 40.0000 ppm. We recorded 2 scans per increment, arriving at a total measuring time of 10 minutes per spectrum. Samples with NPs were intensely vortexed for two minutes just before the measurement, to avoid any possible sedimentation.

For each L-lysine concentration, we recorded a spectrum in the absence and presence of the NPs.

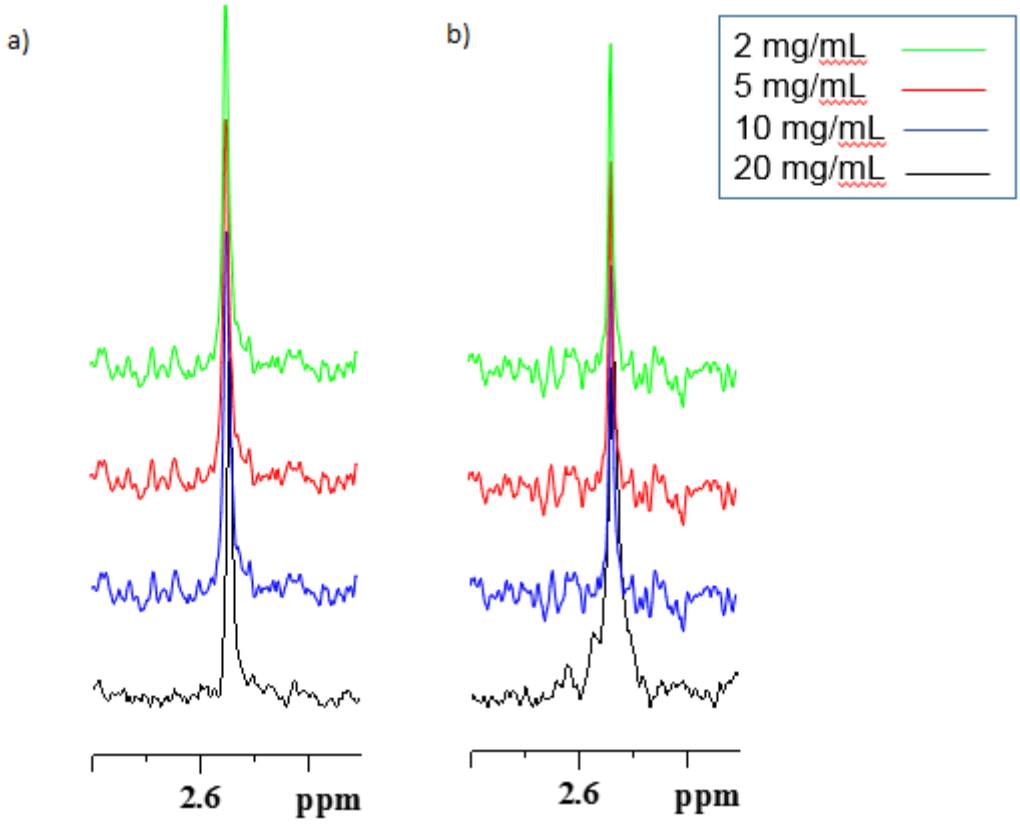

Figure S34. 31P NMR spectra for the Chemical Shift Perturbation measurements with **Ru** (a) and **RuPt-dba** (b) on the L-lysine, decreasing the concentration of lysine, at constant concentration of NPs.

[3] A.G. Palmer III, J. Cavanagh, P.E. Wright, M. Rance, *J. Magn. Reson.* **1991**, *93*, 151-170.

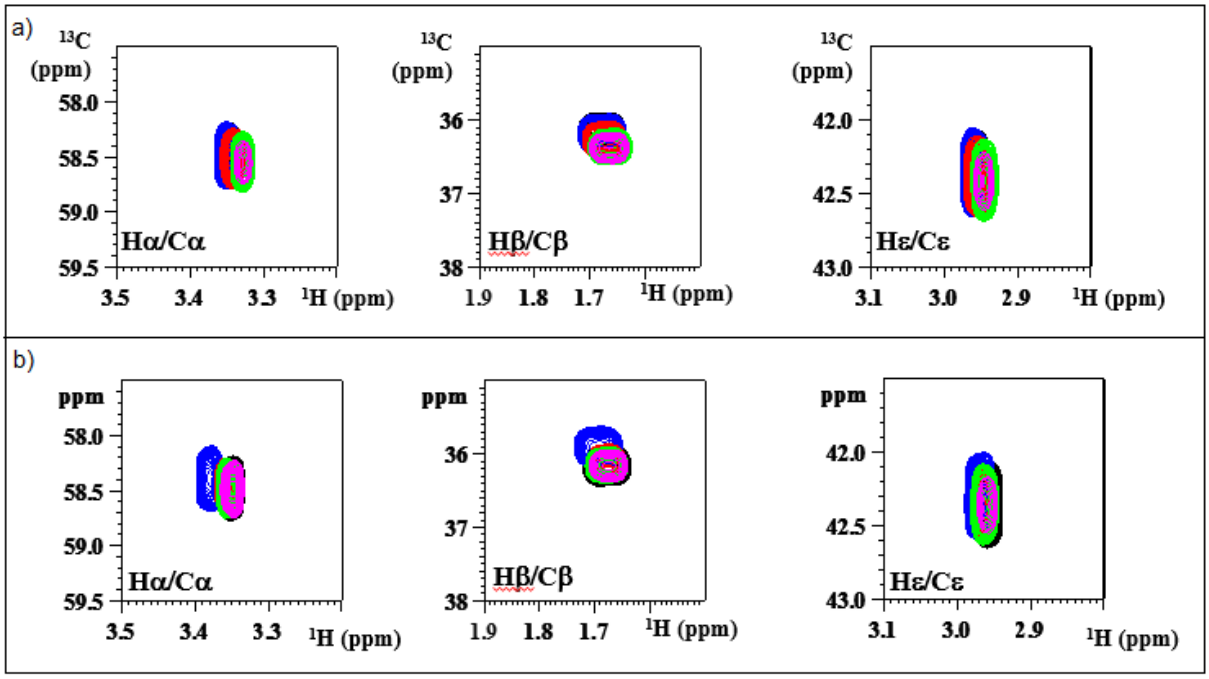

Figure S35. ^{13}C NMR spectra for the Chemical Shift Perturbation measurements with **Ru** (a) and **RuPt-dba** (b) on the L-lysine, decreasing the concentration of lysine, at constant concentration of NPs.

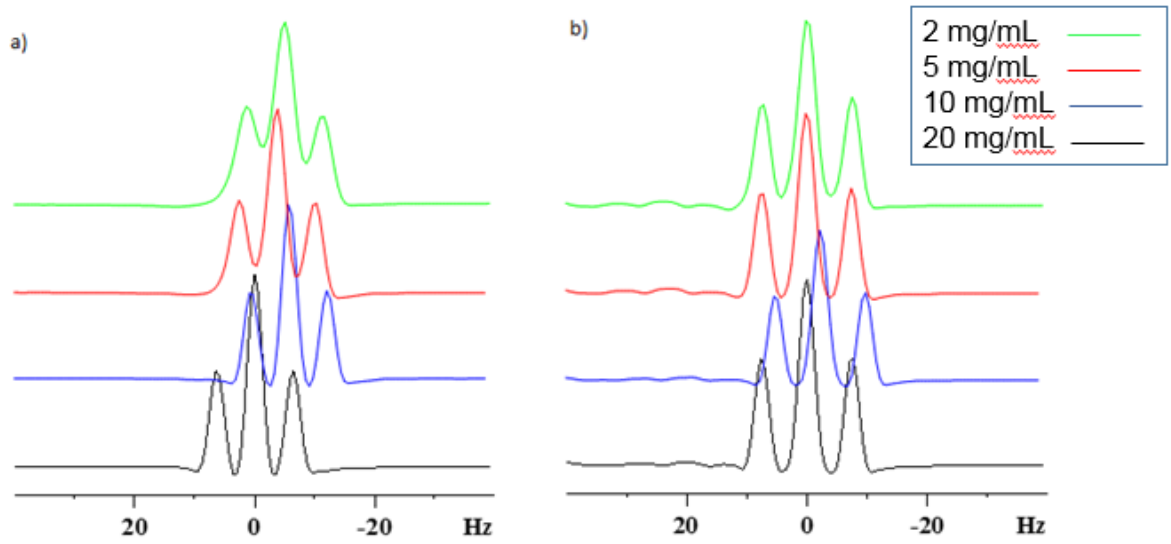

Figure S36. Chemical Shift Perturbation measurements in high resolution proton 1D spectra on the L-lysine (Cα (a) and Cε (b) positions), decreasing the concentration of lysine, without NPs.